Acta Geologica Polonica, Vol. 76 (2026), No. 2, e84
DOI: 10.24425/agp.2026.158198

The uppermost Jurassic–Lower Cretaceous (Tithonian–Aptian) of the Raptawicka Gate section (High-Tatric succession, Poland): integrated stratigraphy and microfacies

DAMIAN GERARD LODOWSKI[1], JUSTYNA KOWAL-KASPRZYK[2], ANNA WAŚKOWSKA[2], BRUNO GRANIER[3] and JACEK GRABOWSKI[1]

[1] *Polish Geological Institute–National Research Institute, ul. Rakowiecka 4, 00-975 Warszawa, Poland; e-mails: damian.lodowski@pgi.gov.pl; jacek.grabowski@pgi.gov*
[2] *AGH University of Krakow, Faculty of Geology, Geophysics and Environmental Protection, Al. A. Mickiewicza 30, 30-059 Cracow, Poland; e-mails: kowalj@agh.edu.pl; waskowsk@agh.edu.pl*
[3] *Muséum d'histoire Naturelle (corresponding member), Route de Malagnou 1, 1208 Genève, Switzerland; e-mail: brcgranier@free.fr*

ABSTRACT:

Lodowski, D.G., Kowal-Kasprzyk, J., Waśkowska, A., Granier, B. and Grabowski, J. 2026. The uppermost Jurassic–Lower Cretaceous (Tithonian–Aptian) of the Raptawicka Gate section (High-Tatric succession, Poland): integrated stratigraphy and microfacies. *Acta Geologica Polonica*, **76** (2), e84.

This study presents the results of research conducted on material coming from the Raptawicka Gate section of the High-Tatric autochthonous succession (Kościeliska Valley, West Tatra Mts, Central West Carpathians, Poland). It utilizes biostratigraphic (calpionellids, calcareous dinocysts, foraminifers), quantitative microfacies, and geochemical (stable carbon and oxygen isotopes, main and trace elements concentrations) techniques. The section documents the transition between the Raptawicka Turnia Limestone (RTL) Fm and the Wysoka Turnia Limestone (WTL) Fm, with an erosional gap in between them. The RTL Fm part contains the Malmica–Remanei microfossil zones, and therefore belongs to the middle lower–upper Tithonian; the WTL Fm part contains a foraminiferal assemblage which characterizes the Barremian/Aptian transition and the lower Aptian, whereas the $\delta^{13}C$ record largely conforms with the characteristics of Oceanic Anoxic Event 1a (OAE 1a). Correlation with the Giewont composite section (High-Tatric allochthonous unit) enables the presentation of a coherent record of Tithonian sedimentation in both areas. It also allows the inference that the topmost beds of the RTL Fm in the Raptawicka Gate section are younger than those in the Giewont composite section. Furthermore, the stratigraphic gap between the topmost Jurassic and the Lower Cretaceous sediments in the High-Tatric autochthonous cover (Raptawicka Gate) is significantly larger (topmost Tithonian–basal Aptian) than that within the Giewont Nappe (cf. topmost Tithonian–Berriasian). Ultimately, microfacies analysis allows the recognition of biotic events/processes documented in other western Tethys sections; these are thought to reflect major-scale environmental perturbations.

Key words: Central Western Carpathians; Tatra Mountains; Kościeliska Valley; Carbonates; Calpionellids; Foraminifers; Carbon isotopes.

INTRODUCTION

The stratigraphy of the uppermost Jurassic–Lower Cretaceous (Tithonian–Hauterivian) of the Lower Sub-Tatric succession in the Tatra Mts is quite well recognized due to the application of micro- and nannofossil stratigraphy, magnetostratigraphy and chemostratigraphy (Pszczółkowski 1996, 2003; Grabowski and

Pszczółkowski 2006; Grabowski *et al.* 2025). On the contrary, the stratigraphy of the Jurassic–Cretaceous (J/K) transition interval in the High-Tatric succession is not as clear, as it consists of relatively shallow-water carbonates, poor in diagnostic microfossils and clastic admixture (Lefeld 1968). However, the development and improvement of research techniques has ultimately enabled relatively precise dating and further palaeoenvironmental interpretation of the J/K transition in the Giewont succession (Pszczółkowski *et al.* 2016; Pszczółkowski 2018; Lodowski *et al.* 2022a; Lodowski and Grabowski 2023).

This study aims to investigate the stratigraphy, microfacies, and stable carbon and oxygen isotopes of the Upper Jurassic–Lower Cretaceous carbonates of the Raptawicka Gate section (Kościeliska Valley, West Tatra Mts, Poland), in the autochthonous part of the High-Tatric succession. The data collected are compared with those obtained from the Giewont composite section, and they are subsequently correlated with the general uppermost Jurassic–Lower Cretaceous stratigraphic framework, as documented in the basinal sections (i.e. Grabowski *et al.* 2019; Lodowski *et al.* 2025).

GEOLOGICAL SETTING

The Tatra Mountains are located in the northernmost part of the Central Western Carpathians, a part of the vast Alpine-Carpathian-Dinaric orogen (Text-fig. 1). The Tatras are composed of a crystalline core and uppermost Paleozoic–Mesozoic and Palaeogene sedimentary covers. The crystalline basement consists of the granitoids of the High Tatra Mts, as well as the granitoid and metamorphic rocks of the Western Tatra Mts, whereas the sedimentary cover consists of: 1) High-Tatric autochthonous and parautochthonous cover and High-Tatric nappes; as well as 2) Sub-Tatric nappes (for details see e.g. Jurewicz 2005 and references therein). In the latest Jurassic/earliest Cretaceous plan, the High-Tatric sedimentary zone was located on the so-called South Tatric Ridge. The South Tatric Ridge, along with the North Tatric Ridge, and the Šiprúň Basin in between, accounted for the so-called Tatricum (micro)terrain (Text-fig. 1F), which faced the Vahic Ocean (part of the Penninic-Ligurian-Vah oceanic system) to the north and the Zliechov Basin (sedimentary zone of the Sub-Tatric nappes) to the south (i.e. Häusler *et al.* 1993; Plašienka 2018 and references therein).

The area of this study — the Raptawicka Gate section — is located within the High-Tatric autochthonous zone (see Kotański 1971; Piotrowski 1978; Szczegółowa Mapa Geologiczna Tatr 2022). The Raptawicka Turnia Limestone Formation (RTL Fm), which predominantly accounts for the Upper Jurassic of the High-Tatric sedimentary zone, can be subdivided into three informal members: 1) pinkish pelitic limestones with ammonites (lower member, Callovian–Oxfordian); 2) light gray *Saccocoma*-cyanoid limestones (middle member, Oxfordian–lower Tithonian); and 3) nearly black cyanoid limestones (upper member, Tithonian) (Lodowski *et al.* 2022a; see also Lefeld 1968; Lefeld *et al.* 1985). Recently, Lodowski *et al.* (2022a) documented that, within the High-Tatric Giewont Nappe, the RTL Fm is erosively cut by a latest Tithonian–Berriasian disconformity. There, the RTL Fm is followed by upper Berriasian–lower Valanginian lithoclastic limestones and — after another lacuna — upper Valanginian (?and Hauterivian) encrinites, both assigned to the Wysoka Turnia Limestone Formation (WTL Fm; Lefeld 1968; Lodowski *et al.* 2022a). Somewhat enigmatic remains the issue of the dating of the Lower Cretaceous encrinites of the Wysoka Turnia Limestone Fm. In addition, the presence of the stratigraphic gap between the Jurassic and Cretaceous has been documented so far only in the Giewont succession, whereas stratigraphic continuity between the Tithonian and Berriasian was previously postulated in the entire High-Tatric domain (Lefeld 1968; Madzin *et al*., 2014; Borowska 2015).

Section description

The Raptawicka Gate section provides an insight into the record of the uppermost Jurassic–lowermost Cretaceous of the High-Tatric autochthonous sedimentary cover. It is located in the middle part of the Kościeliska Valley, ca. 4 km south of its mouth. The base of the succession is located at 49°14’23” N, 19°51’50” E. It consists of the generally northerly dipping (approximated dip direction is 20/50 N, see also Grabowski 1997) dark gray cyanoid limestones of the RTL Fm and the overlying light gray calcarenites of the Giewont Member of the WTL Fm. These outcrop on the western side of the Kościeliski Stream, in between the entrance to the Kraków Gorge and the exit way from Mylna Cave (Text-fig. 1). The section was described in detail by Lefeld (1968), who accounted for both stratigraphic continuity across the J/K transition and the Valanginian age of the uppermost part of the RTL Fm. An updated description of the section and a provisional stratigraphic re-interpretation has been provided recently by Grabowski *et al.* (2022). The total thickness of the investigated interval is around

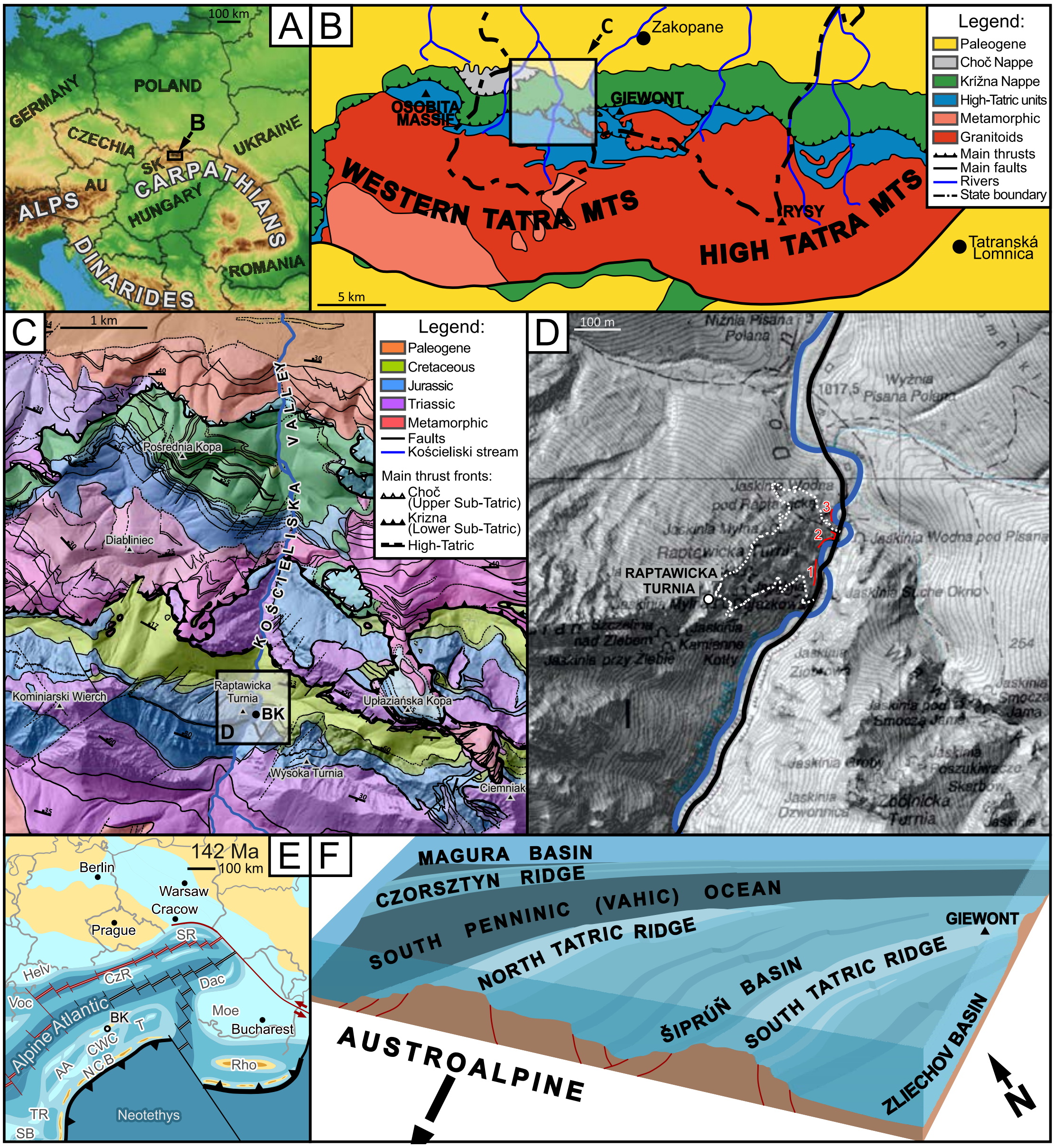

Text-fig. 1. Geological setting of the study area. A) Location of the Tatra Mountains in Europe; Abbreviations: AU – Austria; SK – Slovakia. B) Geological map of the Tatra Mts (modified after Nemčok *et al.* 1994 and Jurewicz 2005). C) Geological map of the Kościeliska Valley (modified after Grabowski *et al.* 2022). D) localization of the studied section in the vicinity of the Raptawicka Gate; numbers next to red lines indicate lower, middle and upper segments of the section, respectively. E) Simplified paleogeographic map of the Alpine Atlantic area during the Berriasian (modified after Lodowski *et al.* 2025). Abbreviations: AA – Austro Alpine; CWC – Central Western Carpathians; NCB – Neotethyan Collision Belt; CzR – Czorsztyn Ridge (Pieniny Klippen Belt); Helv. – Helvetic units; Moe – Moesian Platform; Rho – Rhodopes; SB – Slovenian Basin; SR – Silesian Ridge; T – Tisia; TR – Transdanubian Range; Voc – Vocontian Basin. F) Conceptual paleogeographic reconstruction of the Tatricum and adjacent area during the latest Jurassic; as in Lodowski and Grabowski (2023).

94 meters (Text-fig. 2); however, due to two observational gaps and poorly constrained bedding (Piotrowski 1978), the actual thickness should be treated as approximate. The section starts with massive dark grey limestones, which continue up to the 69.5 m horizon. Within this interval, a ca. 10 m thick observational gap occurs between meters 32 and 42. The dark grey limestones are followed by light gray, in places brownish calcarenites (69.5–73 m). Above meter 73 there is another ca. 10 m thick observational gap, above which

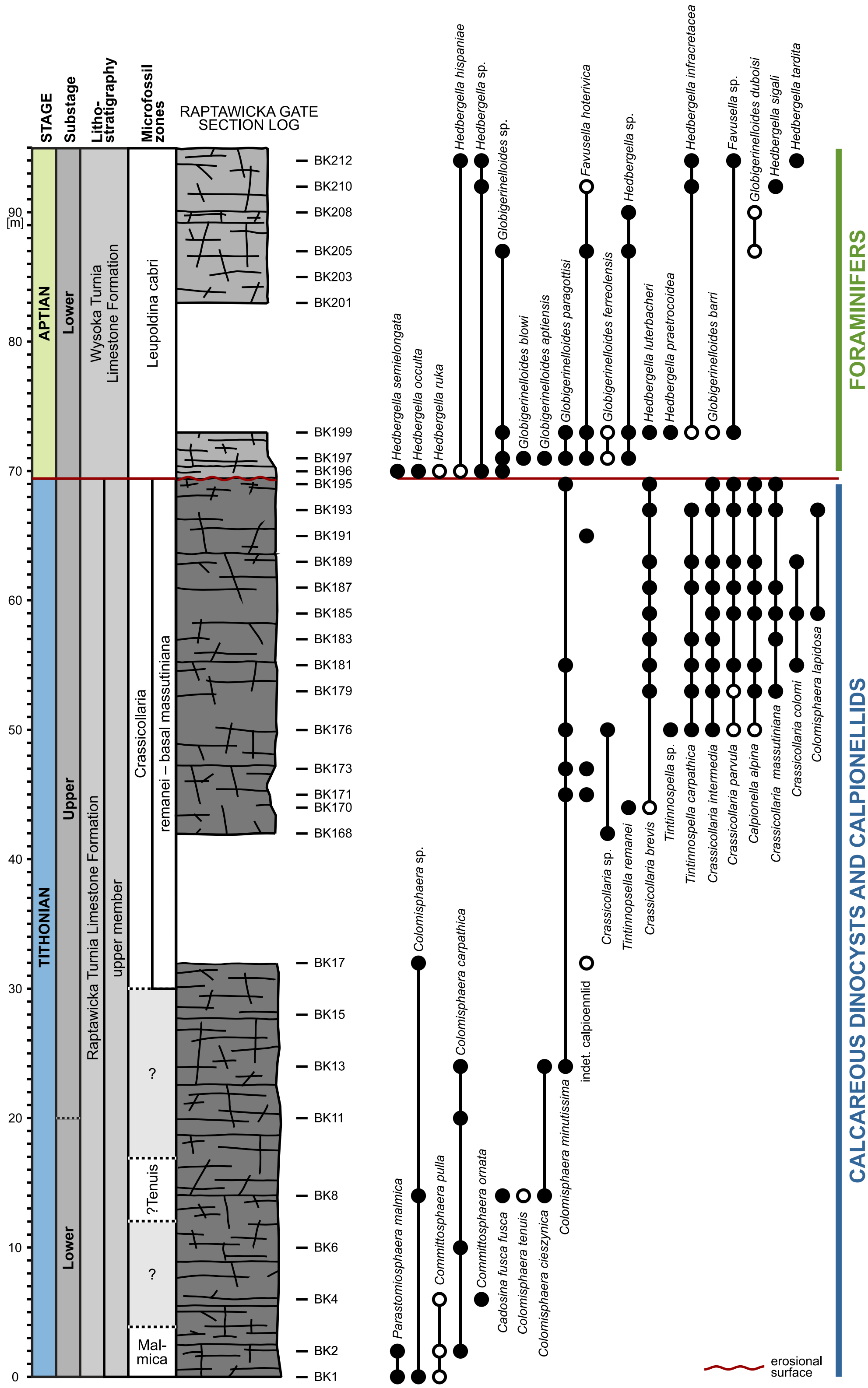

Text-fig. 2. Stratigraphy of the Raptawicka Gate section and microfossil range charts: calcareous dinocysts and calpionellid within the Tithonian and planktic foraminifers within the lower Cretaceous. Dashed lines indicate uncertain boundaries. Empty circles indicate taxa determinated as *conformis*.

massive light gray calcarenites continue up to the top of the section (83–94 m) (see also Appendix 1).

METHODS

This study involves data obtained during two field campaigns which were carried out in 2014 and 2023. The resultant biostratigraphic framework utilizes data collected during both campaigns, whereas the quantitative microfacies analysis and geochemical analyses rely solely on the second campaign material. Investigations were fully integrated, that is the same samples were used for different kinds of analysis. All the numerical data are provided in tabular form (as .xlsx file) in an Appendix 2.

Microfossil biostratigraphy and microfacies analysis

This study investigates a total number of 32 thin sections for the purposes of calpionellid and calcareous dinocyst stratigraphy, as well as microfacies analysis. The calpionellid zonation of Lakova and Petrova (2013), and calcareous dinocyst zonation after Reháková (2000) were applied. The age of the upper part of the section was established using planktic foraminifera (inspected in thin section images) and the zonation of Petrizzo *et al.* (2024) and references therein; additional information was taken from benthic foraminifers observed in thin sections.

Microfacies analyses were performed based on thin section scan images taken with a Keyence VHX-7000 series microscope (Polish Geological Institute–National Research Institute, PGI–NRI); each picture was taken with the same magnification. Microfacies analysis was performed on a representative area of the thin section using JMicroVision software. In each sample coming from the RTL Fm one thousand points were counted and assigned to one of the following groups: micrite matrix, spar/microspar, lithoclasts, cyanoids, cortoids, peloids, oncoids, dinoflagellata cysts, calpionellids, saccocomids, other crinoids, radiolarians, *Globochaete alpina* algae, planktic foraminifers, benthic foraminifers, bivalves, ammonites, other detritus; in case of the WTL Fm (encrinite) samples only 500 points were examined.

Additionally, all thin sections which contained cyanoids were subjected to cynoid morphometry measurements (see Lodowski and Grabowski 2023). The largest and smallest axis of each cyanoid was measured (x-axis: largest; y-axis: smallest); a total number of 1533 grains was evaluated. These measurements were later used for calculations of mean cyanoid size (= mean value of the x-axis) and ellipticity (= x-axis / y-axis).

Magnetic susceptibility and geochemical analyses

A set of 62 samples was subjected to magnetic susceptibility (MS) investigations. Mass-normalized MS measurements were processed using Agico MFK1-FB kappabridge and Safyr 7 software (Paleomagnetic Laboratory of the PGI–NRI).

The same samples were also subjected to measurements of elemental concentrations, obtained through X-ray fluorescence (XRF) spectroscopy using the Olympus Vanta spectrometer (PGI–NRI). However, very low concentrations (often near or below the detection limit) of elements such as Al, K, Ti, and Th (typically considered as detrital, see e.g., Calvert and Petersen 2007) translate into their poor statistical correlation. On this basis, this study considers only Ca content, which acts as a function of carbonate productivity.

Ultimately, stable carbon and oxygen isotope analyses were conducted on 23 carbonate powder samples which were reacted with 100% phosphoric acid at 70°C using a Gasbench II connected to a ThermoFischer Delta V Plus mass spectrometer at the GeoZentrum Nordbayern (Germany). Oxygen and carbon isotope values are reported in per mil relative to the VPDB scale by calibration to the accepted values of NBS 19 ($\delta^{13}C$ = +1.95‰; $\delta^{18}O$ = -2.20‰) and LSVEC ($\delta^{13}C$ = -46.6‰; $\delta^{18}O$ = -26.7‰) references. The reproducibility of the measurements was monitored over the course of analyses by replicated analyses of laboratory standards Erl-5 (n = 12), and Sol-2 (n = 12), as well as the international standard IAEA 603 (n = 6). Reproducibility for $\delta^{13}C$ and $\delta^{18}O$ values was 0.06 and 0.04‰ (±1σ) for Erl-5, 0.04‰, and 0.04‰ (±1σ) for Sol-2, as well as 0.02‰ and 0.06‰ (±1σ) for IAEA 603, respectively.

RESULTS

Biostratigraphy of the Raptawicka Gate section

Calcareous dinocysts and calpionellids

The thin sections coming from the Raptawicka Gate are in general poor in diagnostic microfossils (Text-fig. 2; Plate 1). In the lowest samples (BK1 and BK2) the calcareous dinocyst *Parastomisphaera malmica* (Borza) is relatively common, suggesting the

Malmica Zone (middle part of the lower Tithonian). Samples BK4, BK6, BK11, BK13, BK15 are barren in biostratigraphically important forms, yet the occurrence of *Saccocoma* sp. and such calcareous dinocysts as *Colomisphaera carpathica* (Borza), *Colomisphaera cieszynica* Nowak (sample BK8), *Committosphaera* cf. *pulla* (Borza) confirm the Tithonian age. In the sample BK8 rare specimens of *Colomisphaera* cf. *tenuis* (Nagy) may suggest the Tenuis Zone and the lower/upper Tithonian transition. The first rare and poorly preserved calpionellids appear in sample BK17, in BK168 the first *Crassicollaria* sp. can be recognized, and in sample BK170 – *Tintinnopsella remanei* Borza. Calpionellid assemblages are relatively well developed in samples BK176–BK195. *Crassicollaria intermedia* (Durand Delga) dominates, however in upper samples the amount of *Crassicollaria brevis* Remane and *Crassicollaria parvula* Remane increases. *Crassicollaria colomi* Doben and *Crassicollaria massutiniana* (Colom) remain rare. Gradually *Calpionella alpina* appears more often, but it is represented only by small and medium-sized forms.

Foraminiferal assemblage

Benthic foraminifers occur sporadically and in most cases they cannot be determined to the species level. In samples BK196–BK212 there were documented forms from the genera *Dorothia*, *Gaudryina*, *Conorboides*, *Valvulineria*, *Haplophragmoides*, *Bovilinopsis*, *Glomospira*, *Belorussiella*, *Lenticulina* as well as single miliolids. Characteristic is the occurrence of undeterminable orbitolinids in samples BK196 and BK201. Only four specimens of *Nezzazata isabellae* (BK208 and BK210, three with *conformis* assignment), one *Protopeneropolis banatica* (BK210) and one *Sabaudia* ex gr. *minuta* (BK210) might have been assigned at the species level (Text-fig. 2; Plate 2).

Planktic foraminifera are generally rare and usually occur as isolated and dispersed specimens. They are more frequent within the lower part of the studied interval of the WTL Fm (BK196–BK212), and become even more sporadic upwards. The state of preservation is moderate to poor; the foraminiferal tests are often deformed or affected by recrystallization, which limits detailed taxonomic identification. A hedbergellid–globigerinelloides assemblage composed of cosmopolitan forms is typical for the Barremian–Aptian (Text-fig. 2; Plate 3). Accordingly, sample BK196 contains *Hedbergella hispaniae* Longoria, *H. occulta* Longoria, *H. semielongata* Longoria, and *H.* cf. *ruka* (Banner, Copestake et White). In sample BK197 were found *Favusella hoterivica* (Subbotina), *Globigerinelloides aptiensis* Longoria, *G. blowi* (Bolli), and *G. paragottisi* Verga et Premoli Silva. *F. hoterivica* (Subbotina), *Globigerinelloides aptiensis* Longoria, *Globigerinelloides* cf. *barri* (Bolli, Loeblich et Tappan), *Globigerinelloides paragottisi* Verga et Premoli Silva, *Hedbergella infracretacea* (Glaessner), *Hedbergella luterbacheri* Longoria and *Hedbergella praetrocoidea* Kretchmar et Horbachik characterize sample BK199. Above, in sample BK205 were found *F. hoterivica* (Subbotina) and *Globigerinelloides* cf. *duboisi* (Chevalier), while in BK208 occurs *G.* cf. *duboisi*. Sample BK210 accounts for *F.* cf. *hoterivica* (Subbotina), *H. infracretacea* (Glaessner) and *Hedbergella sigali* Moullade. Ultimately, in sample BK212 there occur *H. infracretacea* (Glaessner), *H. hispaniae* (Longoria) and *Hedbergella tardita* (Antonova) (see Text-fig. 2).

Microfacies succession

The Raptawicka Gate section starts with bioclastic wackestone with lithoclasts (BK1; 0 m), characterized by a relatively low amount of coated grains (cyanoids, cortoids; <2%) (Text-fig. 3). Lithoclasts are small (usually below 1 mm in diameter), rounded and often have a darker, cortoid-type coating. In terms of microfacies and fossil assemblage they resemble the host rock; most likely they document early post-depositional subaqueous erosion (soon after lithification) and intra-basinal reworking, i.e. due to waving processes. The percentage of coated grains (most of all cyanoids) gradually increases up to 40% in sample BK168 (42 m), accounting for a succession of cyanoid packstones with lithoclasts (BK2–BK6; 4–12 m), bioturbated cyanoid wackestones/packstones (BK8–BK11; 16–20 m) and cyanoid packstones (BK13–BK168, 24–42 m). Above, the relative share of cyanoids in thin sections starts to decrease, down to ~4.5% in sample BK187 (61 m), which corresponds with the cyanoid-lithoclastic packstones (BK170–BK179; 44–53 m) and cyanoid-lithoclastic packstones/wackestones (BK181–BK187; 55–61 m). Although cyanoids are abundant again above (ca. 24% in sample BK189, 63 m; ca. 30% in sample BK195, 69 m), sample BK191 (65 m) comprises wackestone barren in cyanoids, while in sample BK193 (67 m) they constitute only ~9% (Text-figs 3 and 4). The entire interval described above is included in the Raptawicka Turnia Limestone Formation (see Lefeld *et al.* 1985). In this context, the unusual (relative to other RTL samples) characteristics of sample BK191 (Text-fig. 4.5) most likely document calmer sedimentation within a seafloor cavity, into which cyanoids could not have been transported or formed there.

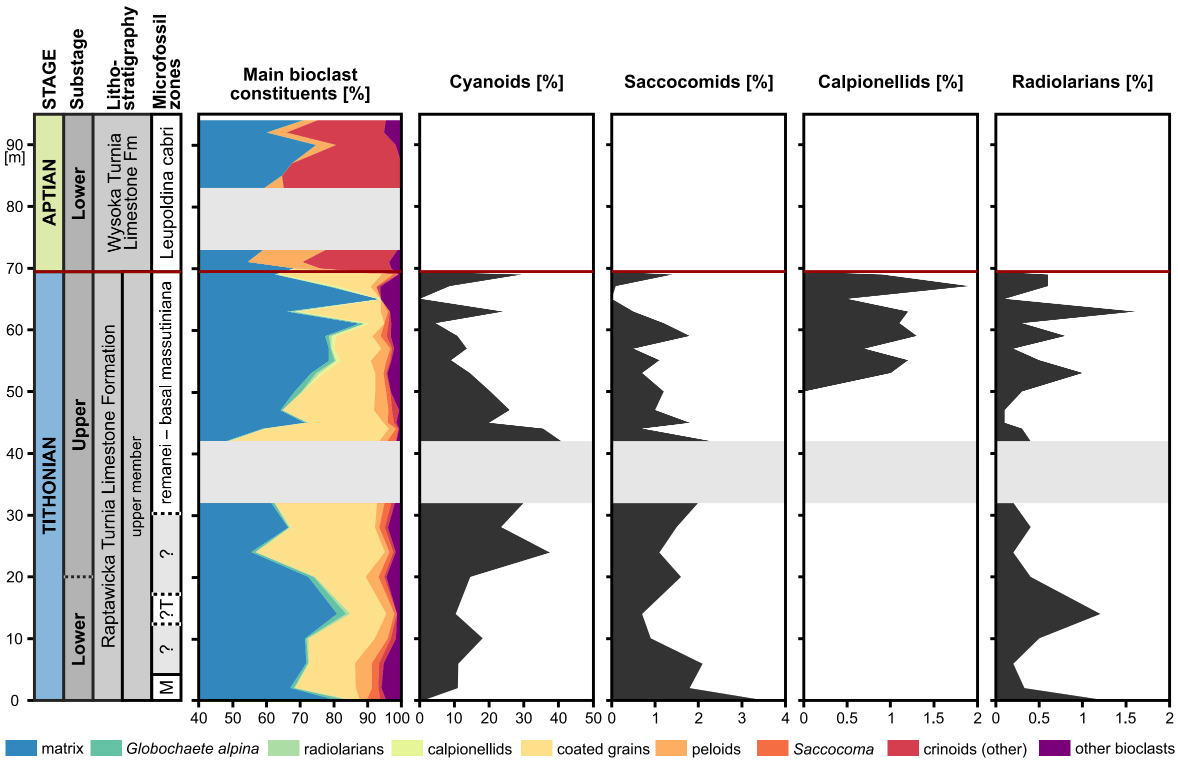

Text-fig. 3. Relative share of selected groups of bioclasts in the Raptawicka Gate section. Abbreviations: M – Malmica Zone; T – Tenuis Zone. Solid red line indicates erosive contact between the RTL and WTL formations. Gray belts indicate observational gaps.

A sudden microfacial change can be observed between samples BK195 (69 m) and BK196 (70 m). Sample BK196 (70 m) represents a packstone with crinoids, orbitolinids and planktic foraminifers (Text-fig. 4.7). Noteworthy, it also contains intraclasts, which in terms of microfacial characteristics are to a large extent a reminder of the RTL Fm (Appendix 3), therefore they are thought to document erosion of the RTL Fm. The following beds (samples BK197–BK199; 71–73 m) are clearly dominated by encrinites (ca. 20–25%) and peloids (~16–19%), as well as accessory foraminifers. The topmost part of the section, above the observational gap (samples BK201–BK212 (83–94 m) is also dominated by crinoidal elements (16–36%) with admixture of peloids (~0–6%) and other bioclasts (~0–5%); in sample BK201 also orbitolinids were documented (Text-figs 3 and 4).

Such a quantitative approach to microfacies analysis allows the observation of variations in the share of different classes of bioclasts, not only the relative dominance of main rock constitutents (cyanoids and crinoids). Characteristic is the sudden increase in relative numbers of calpionellids; their loricas are absent between 0 and 28 m of the section (samples BK1–BK15), and very rare between 32–50 m (BK17–BK176). In the topmost part of the RTL Fm (BK179–BK195; 53–69 m), their number increases to an average of ~1% and a maximum of 1.9% (BK193, 67 m) (Text-fig. 3).

The other characteristic phenomenon is the generally decreasing amount of *Saccocoma* elements, which commonly constitute the nuclei of cyanoids. At the base of the section (BK1, 0 m) saccocomids account for ~3.5% of rock volume; they become less common (<1%) already in samples BK6–BK8 (12–16 m), yet their numbers increase above, reaching > 2% in sample BK168 (42 m). The following beds (BK170–BK195, 44–69 m) account for another successive decline of *Saccocoma* (Text-fig. 3); this may reflect the process of their disappearance, which is usually observed around magnetozone M19r (cf. basal Massutiniana or Intermedia calpionellid subzones; see Lodowski *et al.* 2022b, 2025).

Ultimately, radiolarians are relatively common (0.5–1.6%) within the 53–69 m interval (BK179–BK195), while not being that rare in the lower part of the section (~0.2–0.4%, above 1.2% in samples BK1 and BK8) (Text-fig. 3).

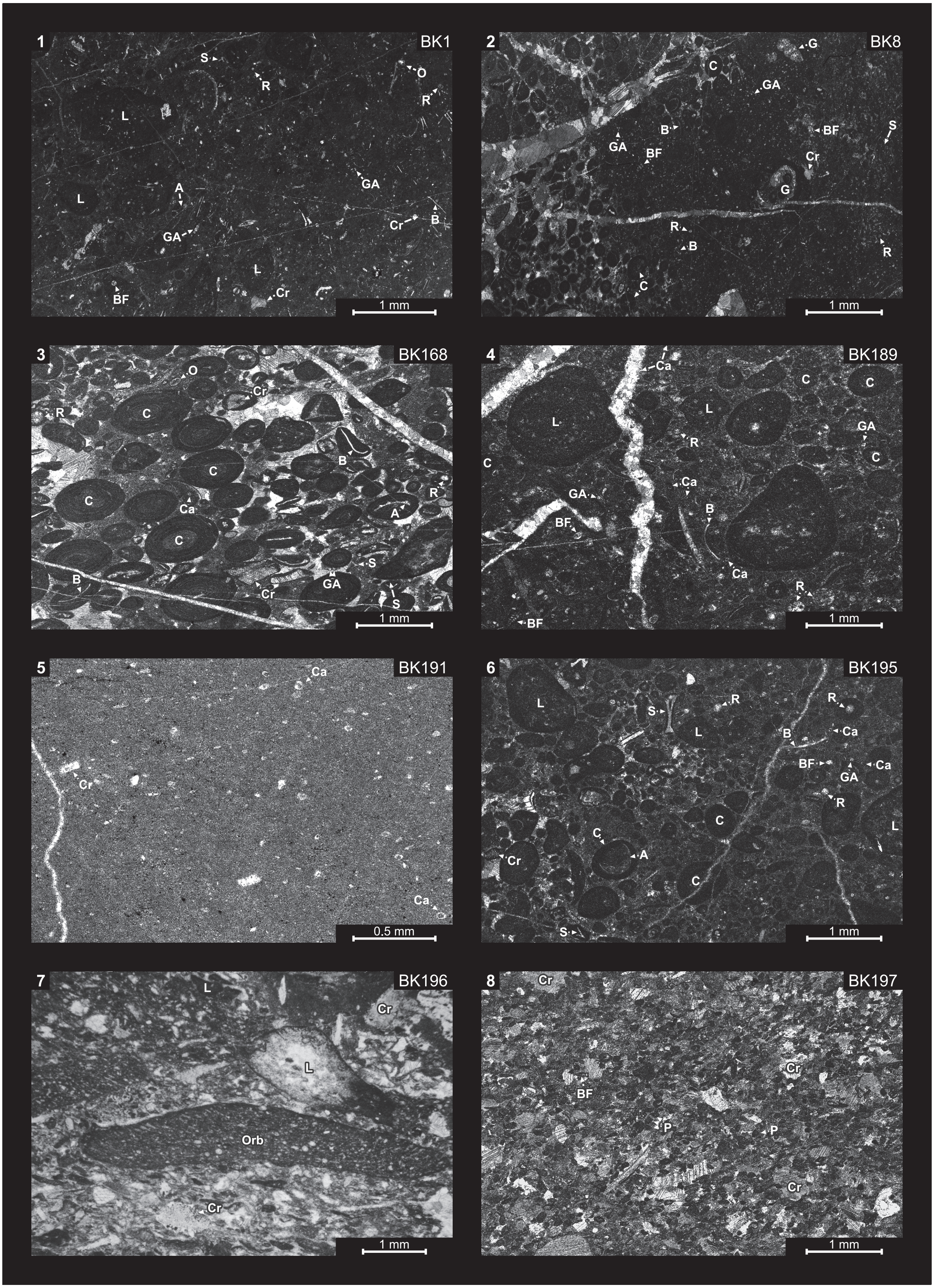
1
BK1
S
O
R
R
L
L
A
GA
GA
Cr
B
L
BF
Cr
1 mm
2
BK8
G
C
GA
B
BF
S
GA
BF
Cr
G
R
B
R
C
1 mm
3
BK168
O
Cr
R
C
C
B
C
Ca
R
A
C
S
B
Cr
GA
S
1 mm
4
BK189
Ca
L
L
C
C
R
GA
C
C
Ca
GA
B
BF
Ca
R
BF
1 mm
5
BK191
Ca
Cr
Ca
0.5 mm
6
BK195
L
S
R
R
L
B
Ca
BF
GA
Ca
R
C
L
C
A
Cr
C
S
1 mm
7
BK196
L
Cr
L
Orb
Cr
1 mm
8
BK197
Cr
Cr
BF
P
P
Cr
1 mm

← Text-fig. 4. Microfacies of the Raptawicka Gate section. 1 – lithoclastic wackestone (sample BK1; 0 m); 2 – bioturbated cyanoid wackestone/packstone (BK8; 14 m); 3 – cyanoid pakstone (BK168; 42 m); 4 – bioclastic-lithoclastic packstone with cyanoids (BK189; 63 m); 5 – wackestone with calpionellids and other bioclasts (BK191; 65 m); 6 – cyanoid-lithoclastic packstone (BK195; 69 m); 7 – crinoidal-lithoclastic wackestone with orbitolinid (BK196; 70 m); 8 – crinoidal packstone with peloids (BK197; 71 m). Abbreviations: A – ammonite aptychus; B – bivalve; BF – benthic foraminifera; C – cyanoid; Ca – calpionellid; Cr – crinoid; G – gastropod; GA – *Globochaete alpina*; L – lithoclast; O – ostracod; Orb – orbitolinid; P – peloid; R – radiolarian; S – *Saccocoma*.

Morphometry of cyanoids

In case of the Raptawicka Gate section, the majority of cyanoids is smaller than 0.5 mm (Text-fig. 5). Furthermore, morphometric measurements do not indicate any clear general trend in their size, although one may notice a vague, irregular increase. The “mean x” value (size index) increases from ca 0.20 mm up to 0.45 mm between the base of the section and 24 m (BK1–BK13); above, it decreases towards sample BK17 (32 m; 0.17 mm) and increases again right above the observational gap, reaching a maximum value of 0.49 mm in sample BK168 (42 m). The upper part of the RTL Fm accounts for another decrease (0.20 mm at BK175, 50 m) and a subsequent increase towards the top of the formation, except for the lack of cyanoids in bed BK191 (65 m).

Considering the ellipticity index (“meany x/y” value), one can observe that in general cyanoids become more round towards the upper parts of the RTL Fm (Text-fig. 5). Nonetheless, after the initial decrease (from >1.6 to <1.4 in 0–24 m interval), the ellipticity index increases in beds BK17 and BK168 (32 m and 42 m, respectively) to >1.6. Although it decreases to 1.3–1.4 already in the BK170–BK179 interval (44–53 m), above, the ratio becomes more bed by bed variable, ranging between 1.13 (BK187, 61 m) and 1.64 (BK185, 59 m), including the lack of cyanoids in bed BK191 (65 m).

Magnetic susceptibility

The magnetic susceptibility remains very low (near-zero, including negative values) and stable through the lower half of the Raptawicka Gate section (0–44 m) (Text-fig. 6). Above, MS increases significantly reaching its maximum (2.50×10^{-8} m^3 kg) in sample BK 174 (48 m). The following, topmost beds of the RTL Fm (48–69 m) manifest a consecutively decreasing trend. The transition between the RTL and WTL formations does not account for any clear contrast in the MS signal (compare sample BK195 with BK196–BK199, 69–73 m). Ultimately, the interval above the observational gap (83–95 m) starts with slightly negative MS, which increases towards the top of the section, including the extraordinary high record at the top (BK213, 95 m, 7.4×10^{-8} m^3/kg; Text-fig. 6).

Geochemistry

Elemental geochemistry

Among the XRF-measured elemental concentrations, the general characteristic is increasing Ca content in the lower part of the section (from ca. 40% to 45% in samples BK1–BK16, 0–30 m) and the lack of a clear trend above, though single values vary between 36–49% (Text-fig. 6). However, these measurements must be taken as an approximation of trend, since the XRF method typically overestimates Ca content (i.e. Fedeli *et al.* 2024). The potassium content remains relatively stable through the entire section (ca. 0.1%), however slightly elevated values may be observed at the base (0–10 m) and the top of the section (95 m). No clear trend can be observed within the Ti dataset, yet a local minimum can be noticed within the 49–56 m interval; the lack of statistical correlation between K and Ti ($r = 0.05$) hampers the reliability of any further investigations based on those elements. The aluminum and Th contents were usually below detection limit.

Stable carbon and oxygen isotopes

The Raptawicka Gate section starts with relatively stable, only slightly decreasing $\delta^{13}C$ values, from ca. 2‰ VPDB at its base to ca. 1.6‰ VPDB at 44 m (sample BK170). From this level upwards, the section documents consecutively increasing $\delta^{13}C$ values, which continue through the upper part of the RTL Fm (44–69 m) and the investigated part of the WTL Fm (69–95 m), reaching up to 3.6‰ VPDB in the sample BK211 (93 m). Only the topmost sample accounts for a lowered carbon isotope signature (2.7‰ VPDB, BK213, 95 m) (Text-fig. 6).

In case of stable oxygen isotopes, their values are relatively variable and negative. The base of

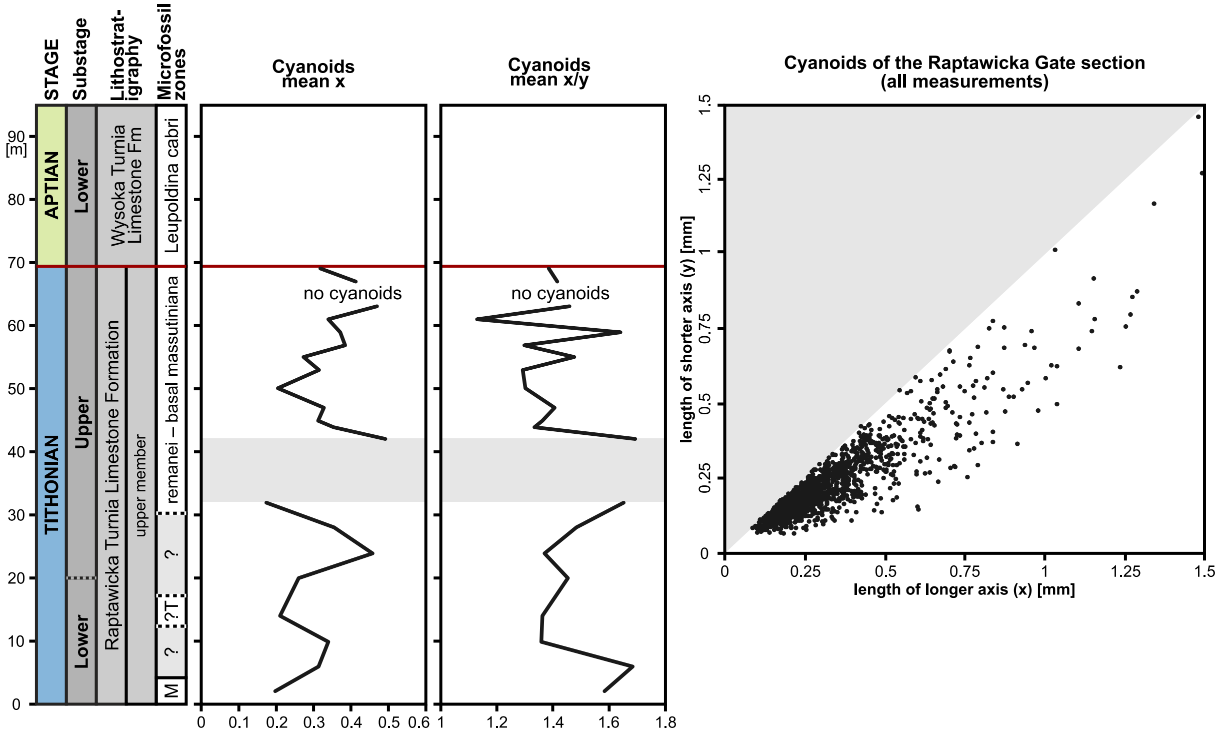

Text-fig. 5. The results of cyanoid morphometry in the Raptawicka Gate section. "Mean x" – size index; "mean x/y" – ellipticity index. Abbreviations as on Text-fig. 3. Gray belts indicate observational gaps.

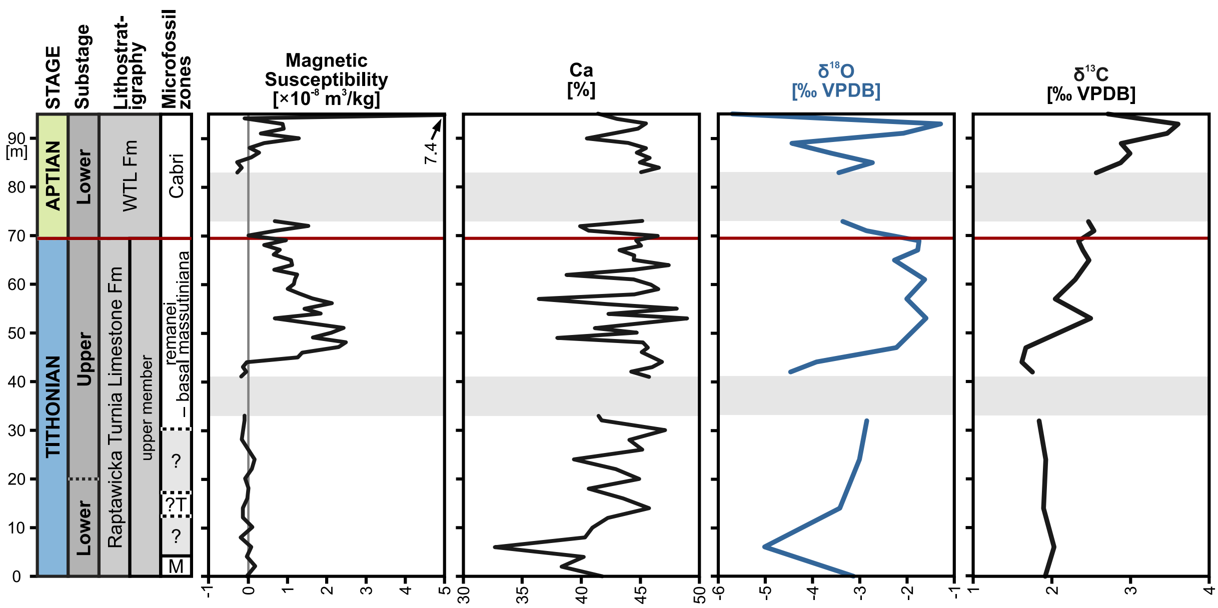

Text-fig. 6. Magnetic susceptibility and portable XRF measured concentrations of Ca, as well as stable oxygen and carbon isotopes in the Raptawicka Gate section. Abbreviations: WTL Fm – Wysoka Turnia Limestone Fm; M. – Malmica; T. – Tenuis. Gray belts indicate observational gaps.

the section (0–8 m) documents a decrease from ca. -3‰ to -5‰ VPDB; δ^{18}O gradually returns to ca. -3‰ VPDB within 8–32 m interval. Above the observation gap, oxygen isotopic signatures are again significantly lighter (ca. -4.5‰ VPDB at 42 m), yet already within the 47–69 m interval they reach near -2‰ VPDB. The WTL Fm interval (70–95 m) provides rather light δ^{18}O (ca. -3‰ VPDB); however, isotopic signatures in the topmost beds are strongly variable, ranging from -1.3‰ (93 m) to -5.7‰ VPDB (95 m) (Text-fig. 6).

Noteworthy, the fact that there is no systematic correlation between δ^{13}C and δ^{18}O (Appendix 4) allows us to exclude diagenesis from factors affecting the carbon isotopic record, at least to a considerable degree (see i.e. Colombie *et al.* 2011). The oxygen isotopes were most likely affected by burial diagenesis as suggested by their highly negative values, much lower than those typical for other Western Tethys sections (compare e.g. with Text-fig. 26.1 in Hesselbo *et al.* 2020; see also Moore 2001).

INTERPRETATION AND DISCUSSION

Stratigraphic framework of the Raptawicka Gate

Calcareous dinocyst occurrences allow the establishment of the base of the Raptawicka Gate section (sample BK1) as belonging to the mid lower Tithonian Malmica Zone, and the BK8 sample (14 m) as probably the lower/upper Tithonian Tenuis Zone (Reháková 2000; Petrova *et al*. 2025). Due to limited micropaleontological data, the continuity of the Tithonian part of the section cannot be reliably established. The Chitinoidella Zone, representing the lowermost calpionellid zone, has not been identified. As calpionellids in the first calpionellid-bearing layers are very rare and unidentifiable, and the first determinable specimens belong to the genus *Crassicollaria* rather than *Tintinnopsella*, it remains unclear also whether the lowermost part of the Remanei Subzone is present. Accordingly, BK17–BK195 beds (32–69 m) can be assigned to the upper Tithonian Crassicollaria Zone — most likely the Tintinnopsella remanei Subzone and the lowest part of the following Massutiniana Subzone (equivalent to the Intermedia Subzone *sensu* Ölveczká and Reháková 2022). In this context, characteristic are relatively numerous calpionellids within the 53–69 m interval (Text-fig. 3), which can reflect the general increase in their number within the topmost Remanei–Massutiniana subzones (see Lodowski *et al*. 2025; Petrova *et al*. 2025). Nonetheless, as large forms of *Calpionella alpina* (cf. *C. grandalpina*) were not observed, the occurrence of the Massutiniana Subzone is not supported biostratigraphically (see Lakova and Petrova 2013).

The occurrence of orbitolinids in sample BK196 and BK201 clearly indicates the early/late Barremian–Aptian age of the upper part of the section (see Simmons and Williams, 1992; Granier *et al.* 2021), corresponding to the so-called High-Tatric "Urgonian" ("reefal" limestones = corals, rudist and orbitolinid bearing carbonates; see Lefeld 1968; Lefeld *et al.* 1985; Michalík and Soták 1990; Michalík, 1994; Masse and Uchman 1997). Furthermore, samples BK197, BK199 and BK205 contain planktic foraminifers *Favusella hoterivica* (Subbotina), which have their last occurrence within the lower Aptian (Premoli Silva and Verga 2004; BouDagher-Fadel 2015) (Leupoldina cabri Zone *sensu* Coccioni *et al.* 2007; Pszczółkowski 2015) (Text-fig. 2). In turn, sample BK196 is estimated as not older than late Hauterivian based on the presence of *Hedbergella semielongata* Longoria, whereas sample BK197 is not older than late Barremian due to the occurrence of *Globigerinelloides blowi* (Bolli) (Coccioni *et al.* 2007; Petrizzo *et al.* 2024). Further stratigraphic information for sample BK196 may provide also the presence of *Hedbergella* cf. *hispaniae* Longoria, the first occurrences of which have been documented from the lower Aptian (Leupoldina cabri Zone; Premoli Silva and Verga 2004; Coccioni *et al.* 2007); nonetheless, this age remains tentative as it relies on *conformis* identification. The topmost part of the section (BK210–BK212) is estimated as early–middle Aptian in age based on the occurrence of typically Aptian taxa, such as *Hedbergella hispaniae* Longoria (see above) and *Hedbergella sigali* Moullade, which (the latter) occurs last in the middle Aptian (Lipson *et al.* 2004; Premoli Silva and Verga 2004; Huber and Leckie 2011; BouDagher-Fadel 2015). However, the co-occurrence of *Favusella* cf. *hoterivica* (Subbotina) may suggest a more specific, early Aptian (Leupoldina cabri Zone) age also for the top of the section. Consequently, the entire WTL Fm interval of the Raptawicka Gate section can be most likely assigned to the lower Aptian, within the Leupoldina cabri Zone, or — more broadly — the Globigerinelloides blowi–Leupoldina cabri zonal transition.

Correlation with other High-Tatric sections

The Giewont section

Correlation between the Raptawicka Gate section (High-Tatric autochthonous unit) and the Giewont composite section (High-Tatric Giewont Nappe; Lodowski *et al.* 2022a; Lodowski and Grabowski 2023) is not straightforward, primarily due to the rather poor biostratigraphic framework of both successions, and the significantly different thicknesses of the upper Tithonian intervals. Accordingly, the upper Tithonian in the Giewont succession is ca. 10 m thick, whereas in the Raptawicka Gate it extends to least 40 m. This implies either a different stratigraphic range of both successions and/or significantly different sedimentation rates.

Considering the MS signal (Text-fig. 7A), characteristic for the Giewont section is a generally increasing trend through the upper Kimmeridgian–lower Tithonian, which is interrupted by a local peak ($>5 \times 10^{-8}$ m^3/kg) within the lowermost Tithonian beds, as well as near-zero values ($\sim 0–1 \times 10^{-8}$ m^3/kg) within the upper Tithonian, except the topmost part of the RTL Fm, where it slightly increases. In turn, the entire lower part of the Raptawicka Gate section (0–45 m) manifests near-zero MS, while only the topmost Tithonian (45–69 m) accounts for elevated MS (up to 2.5×10^{-8} m^3/kg). Accordingly, the lower/upper Tithonian transition in both sections depict different MS values and trends. Consequently, as the magnetic mineralogy of the Giewont area was affected by late diagenesis (oxidation and formation of the superparamagnetic (SP) magnetite; see Lodowski and Grabowski 2023), the near-zero MS signal in the lower part of the Raptawicka Gate can be considered as sedimentary, documenting restricted (near to none) clastic input during the late Tithonian–early Berriasian clastic minimum (see e.g., Lodowski *et al.* 2024b). In this context, the elevated MS values within the topmost Tithonian of the Raptawicka Gate section (45–69 m) are most likely related to local diagenetic imprint. This, combined, prevents the MS-based correlation between the Raptawicka Gate and the Giewont succession.

Morphometric comparison between the Raptawicka Gate section and the Giewont succession is also not obvious (Text-fig. 7B). In the Giewont area, after the initial increase within the Chitinoidella Zone, cyanoids remain relatively large, but also variable in size within the topmost part of the RTL Fm (cf. Crassicolaria Zone) (mean ~0.25–0.45 mm). In this context, the cyanoid size range in the Raptawicka Gate section (mean ~0.2–0.5 mm), along with an only vaguely increasing trend in their size, can be compared with the upper Tithonian cyanoids of the Giewont composite section. Furthermore, increasing size of cyanoids within the upper part of the Remanei–basal Massutiniana Subzone in the Raptawicka Gate section may represent a stratigraphically higher part of the RTL Fm than is exposed within the Giewont section, where the upper Tithonian accounts for only two local cyanoid size peaks (unlike three at Raptawicka Gate). This interpretation may be also supported by the occurrence of wackestone microfacies within the upper Tithonian of Raptawicka Gate (Text-fig. 4.5), which has no analogue in the Giewont succession. Ultimately, the ca. 2‰ VPDB $\delta^{13}C$ values in the lower part of the Raptawicka Gate section (cf. 0–50 m) correlate well with the carbon isotopic signature within the Malmica–topmost RTL Fm in the Giewont composite section. Moreover, the slightly lower $\delta^{13}C$ at 40–45m of the Raptawicka Gate (~1.6‰ VPDB) may correspond with the similar record at the top of the RTL Fm in the Giewont section. (Text-fig. 7C). Accordingly, the increasing carbon isotope trend at the top of the RTL Fm at Raptawicka Gate (cf. 45–69 m) most likely covers the interval absent at the Giewont composite section (as suggested also by cyanoid morphometry; see above). In turn, the consecutive increase in $\delta^{13}C$ within the WTL Fm of the Raptawicka Gate starts with values ~2.5‰ VPDB, therefore already near the maximum values observed within the Giewont Member of the Giewont section (Text-fig. 7C). Consequently, taking into account also biostratigraphic data, the WTL Fm interval in the Raptawicka Gate section (lower Aptian) postdates the WTL Fm interval documented in the Giewont section (cf. upper Valanginian–Hauterivian; note i.e. the lack of orbitolinids and the presence of the foraminifers *Praedorothia praehauteriviana*, *Protomarssonella kummi*, *Uvigerinammina* cf. *uvigeriniformis*, as well as the small gastropod *Pseudonerinea* cf. *vaceki* in the Giewont succession; Lodowski *et al.* 2022a).

The Wysoka Turnia section

The Wysoka Turnia section is the best so far studied Barremian–Aptian section of the WTL Fm in the High-Tatric succession. A detailed litho- and biostratigraphic description of the section was provided by Masse and Uchman (1997). The lower part of the section, which consists of micritic limestones intercalated with three packets "units" U1–U3) of bioclastic limestones with rudist fragments and/or orbitolinids were assigned by the authors to the Raptawicka Turnia Limestone Formation. Masse and Uchman (1997) mentioned that the micritic limestones of the RTL Fm contain micro-oncolites and calcisphaerulids (=most likely cyanoids), *Saccocoma*, *Globochaete*,

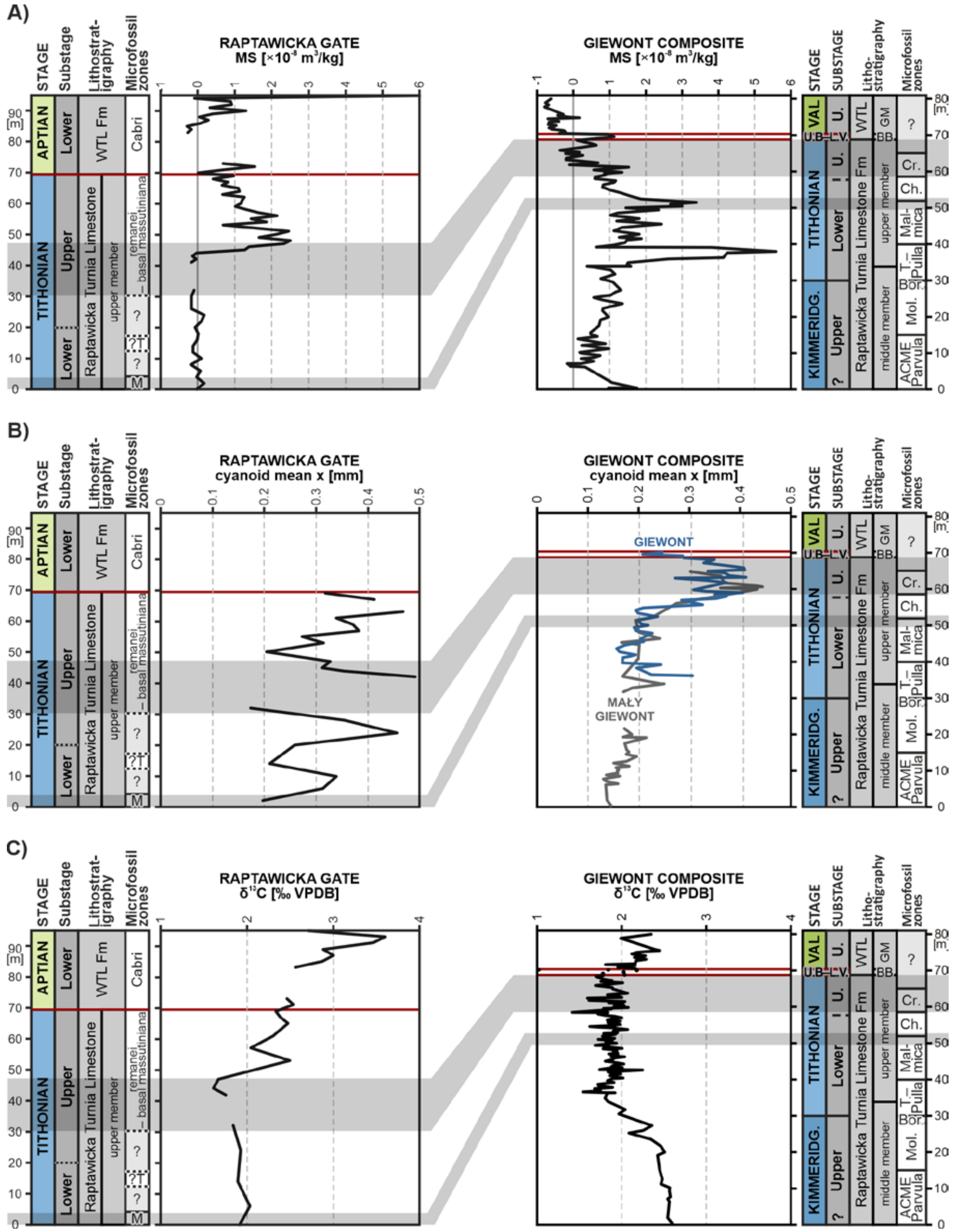

Text-fig. 7. Comparison of different environmental indices in the Raptawicka Gate (this study) and Giewont composite section (Lodowski and Grabowski 2023; Lodowski *et al.* 2022a) of the High-Tatric succession. A – magnetic susceptibility; B – cyanoid size index; C – stable carbon isotopes. Gray belts indicate correlation intervals. Note the lack of the uppermost Tithonian–lower Berriasian in the Giewont composite section. Abbreviations: BER – Berriasian; VAL – Valanginian; L. – Lower; U. – Upper; RTL Fm – Raptawicka Turnia Limestone Fm; WTL Fm – Wysoka Turnia Limestone Fm; GM – Giewont member; BB – basal beds; Bor. – Borzai; Cal. – Calpionella; Ch. – Chitinoidella Cr. – Crassicollaria; Mol. – Moluccana; T. – Tithonica.

and occasional ammonites, however they did not provide a detailed microscopic description of micrites below and in between the successive platform-type units (U1–U3). On this basis it cannot be unanimously stated which parts of the Wysoka Turnia section actually meet the description of the RTL Fm. Based on the most recent lithostratigraphic scheme of Lodowski *et al.* (2022), the top of the RTL Fm (upper member) consists of cyanoid limestones (except in the vicinity of the Mount Osobita, where the Sobótka Limestone member occurs; see also Madzin *et al.* 2014). In turn, the succeeding Lower Cretaceous encrinites (documented from the Osobita, Giewont, and now the Raptawicka Gate sections) were assigned to the Wysoka Turnia Limestone Fm; however, intriguingly, this facies was not described from the Wysoka Turnia section.

Consequently, it seems that Masse and Uchman (1997) included to the RTL Fm also the organodetrital limestones of the Giewont member; however, the occurrence of limestones with rudists and orbitolinids within evidently *Saccocoma*-bearing (= Jurassic) cyanoid (oncolithic) limestones is very unlikely. And indeed, according to Lefeld (1968, Fig. 4), the reef breccias of the Wysoka Turnia section intercalate the "organodetrital limestones", which might be compared to the Giewont member *sensu* Lodowski *et al.* (2022). The other important difference is the lack of rudists and corals in the Raptawicka Gate section. This, combined, prevents more detailed and reliable correlation between the Raptawicka Gate and the Wysoka Turnia sections. Nonetheless, assuming that the stratigraphic interpretation of Masse and Uchman (1997) is correct, the WTL Fm interval of the Raptawicka Gate section would most likely correspond with the interval between the U2 and U3 units of the Wysoka Turnia section (Barremian/Aptian transition), with the first orbitolinid occurrence.

Correlation with global carbon isotope stack

One of the most characteristic features of the Raptawicka Gate section is the more than 1‰ increase in $\delta^{13}C$, from ca. 2.5‰ VPDB in sample BK197 (71 m) to 3.6‰ VPDB in sample BK211 (93 m), and a subsequent decrease to ~2.7‰ VPDB at its top (BK213; 95 m). Taking into account the approximated age of the studied interval of the WTL Fm (Leupoldina cabri foraminiferal Zone or — more broadly — the transition between the Globigerinelloides blowi and Leupoldina cabri zones), such an increasing trend and heavy isotopic signatures can be compared only with the: 1) basal Aptian secondary increase in $\delta^{13}C$ (within the magnetozones CM0r–basal C34n; see Frau *et al.* 2018); or — preferably, if it is accepted that the entire WTL Fm interval falls in the Leupoldina cabri Zone – 2) a part of the early Aptian OAE 1a event *sensu largo* (i.e. Erba *et al.* 1999; Herrle *et al.* 2015; Frau *et al.* 2018; see also Cramer and Jarvis 2020; Gale *et al.* 2020) (Text-fig. 8). In the latter case, the lack of the characteristic sudden drop in stable carbon isotopes, which precisely marks the OA1a event, might be explained by the observational gap occurring between samples BK199 and BK201 (73–83 m).

Tracing the palaeoenvironmental phenomena at the Jurassic–Cretaceous transition

Microfossil turnovers

A substantial bioclastic component of the Tithonian of the Raptawicka Gate section are cyanoids. However, such facies is not the most widespread one amongst the uppermost Jurassic of the Western Tethys (for references see i.e. Mišík 1966, and Mišík and Reháková 2009), therefore any regional and supra-regional comparisons require a focus on other microfossil groups, which have been studied so far in a more detailed way. Accordingly, in case of the Raptawicka Gate section, relatively common are also elements of planktic crinoids from the genus *Saccocoma*, calpionellids, radiolarians, *Globochaete alpina* algae and other crinoids (Text-fig. 3; see also Appendix 2).

Although not many quantitative data are available for the Tithonian/Berriasian boundary interval, some apparently supra-regional patterns can be recognized when comparing the microfacies of Raptawicka Gate with the quantitative studies performed in the Clue de Taulanne (Vocontian Basin, France; Lodowski *et al.* 2025) and Torre de' Busi (Southern Alps; Petrova *et al.* 2025) sections. At first, characteristic for the Raptawicka Gate section is a sudden appearance of relatively numerous calpionellids around 50 m of the section; within the Crassicollaria calpionellid Zone (cf. Remanei–basl Massutiniana Subzone; Text-fig. 3). In turn, in the Clue de Taulanne, calpionellids become most common within mid-upper Tithonian, at the Remanei/Massutiniana zonal transition (cf. M20n/M19r magnetozonal transition; see e.g. Lodowski *et al.* 2022b); increasing calpionellid abundance is observed also at the very same interval (M20n/M19r) of the Torre de' Busi section (Petrova *et al.* 2025). Consequently, the calpionellid "bloom" in the Raptawicka Gate section most likely reflects the general calpionellid bloom, as noted in many western Tethys sections.

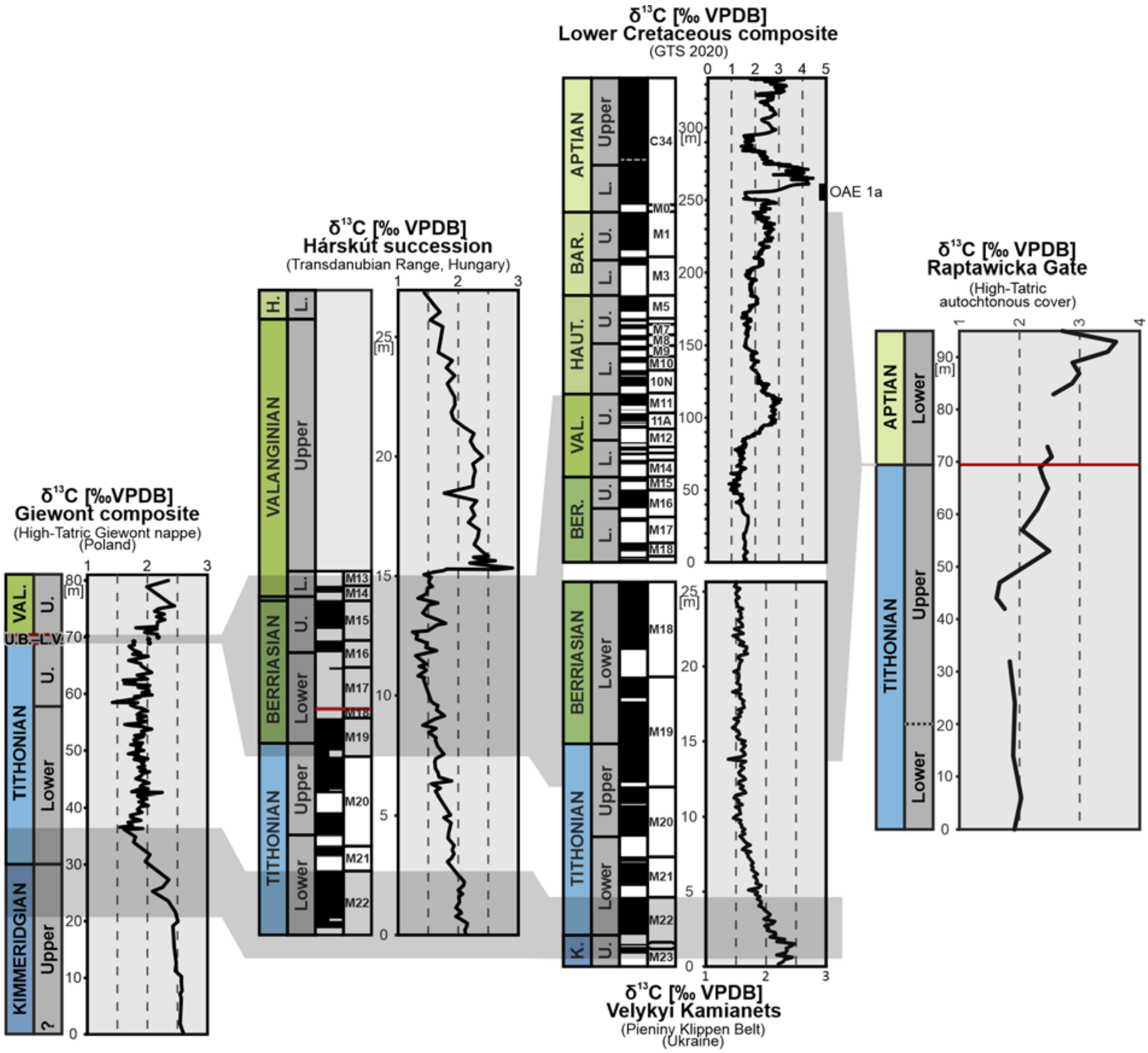

Text-fig. 8. δ13C correlation between the Raptawicka Gate section (this study), Giewont composite section (Lodowski *et al.* 2022a; Lodowski and Grabowski 2023), Transdanubian Range (Hárskút succession, Hungary; Főzy *et al.* 2010; Lodowski *et al.* 2022b), Pieniny Klippen Belt (Velykyi Kamianets section, Ukraine; Grabowski *et al.* 2019) and Lower Cretaceous composite log (Gale *et al.* 2020). Correlative intervals are indicated by gray belts.

The RTL Fm of the Raptawicka Gate section accounts also for common saccocomids, which constitute ~1–2% of rock volume and are present also at the topmost part of the RTL Fm. In the Clue de Taulanne section saccocomids completely disappear from the record within the lower part of the Massutiniana calpionellid Subzone. In turn, in the Hárskút succession (Transdanubian Range, Hungary; Lodowski *et al.* 2022b) elements of *Saccocoma* completely disappear within the magnetozone M19r, which is coherent also with observations performed within the Velykyi Kamianets section (Pieniny Klippen Belt, Ukraine; Grabowski *et al.* 2019). Consequently, even though the topmost part of the RTL Fm in the Raptawicka Gate section covers an interval younger than in the Giewont succession (Lodowski *et al.* 2022a; Lodowski and Grabowski 2023), it most likely still falls within the lower part of the upper Tithonian *sensu* Lakova and Petrova (2023).

The changes in microfossil abundances described above appear to correspond between the three distant sedimentary successions, and they therefore are thought to represent the general biotic response to supra-regional paleoenvironmental processes. In case of the Clue de Taulanne and Torre de' Busi sections, the switch from radiolaria- to calpionella-dominated microfacies was interpreted to be the result of climate changes (cooling and aridization), and related oligotrophication of the sea surface (Lodowski *et al.* 2025). In this context, the calpionellid "bloom" at the topmost part of the RTL Fm is thought to document the same process, yet within the relatively shallow, likely Bahama Bank-type sedimentary zone of the South-Tatric Ridge.

Lower Cretaceous sedimentary gaps in the High-Tatric zone

One of the most characteristic features of the Raptawicka Gate section is the sedimentary gap between the Tithonian and Aptian (Text-fig. 2). So far, the uppermost Jurassic–lowermost Cretaceous sedimentary discontinuities described were from the Giewont succession (Lodowski *et al.* 2022a). There, the first gap was estimated as spanning the uppermost Tithonian–upper Berriasian, whereas the second — following the relatively thin upper Berriasian–lower Valanginian lithoclastic limestones (basal beds of the Giewont Member of the RTL; Lodowski *et al.* 2022a) — accounts for the lower–upper Valanginian. Furthermore, the authors documented the hardground crust at the contact between the upper Tithonian and the upper Berriasian–lower Valanginian interval (see Text-fig. 7 in Lodowski *et al.* 2022a). Later on, as cyanoid morphometry provided unanimous evidence of the Tithonian shallowing trend, the erosional events were interpreted as a result of the interplay between local/regional tectonics and eustasy (i.e. uplift of the South Tatric Ridge and the long-term eustatic regression during the Tithonian–Berriasian; Lodowski and Grabowski 2023). Consequently, the same mechanisms are thought to have controlled deposition (and erosion) in the Raptawicka Gate area. Intriguingly, continuous sedimentation in the Giewont area was reestablished during the late Valanginian (encrinites and carbonates with reefal debris; i.e. Lefeld 1968 and Lefeld *et al.* 1985, confirmed by our own field observations), therefore significantly earlier than in the Raptawicka Gate area (Text-fig. 9). This may be explained by the paleotopography of the South Tatric Ridge; in this case the post- (or syn-)tectonic paleorelief might have affected the timing and duration of erosional processes in different parts of the ridge (see also Lefeld 1968). Noteworthy, the different amount of time covered by stratigraphic gaps in both areas is confirmed biostratigraphically (see chapter Correlation with other High-Tatric sections; see also Lodowski *et al.* 2022a).

Early Cretaceous ("Hauterivian") erosion in the High-Tatric area was considered also by Lefeld (1968, p. 42). However, it must be noted that his stratigraphic framework (also in Lefeld *et al.* 1985) does not meet the current understanding of the uppermost Jurassic–Lower Cretaceous stratigraphy (see Lodowski *et al.* 2022a). At first, the Berriasian and Valaginian *sensu* Lefeld is now known to be in fact Tithonian (compare Lefeld 1968 with Pszczółkowski *et al.* 2016 and Lodowski *et al.* 2022a). Furthermore, the lower part of the "Hauterivian" *sensu* Lefeld (1968; =limited in thickness limestones with tintinnids in pelitic intraclasts, and the following encrinites) most likely corresponds with the basal beds of the Giewont Member (upper Berriasian–lower Valanginian; see Lodowski *et al.* 2022a). Consequently, not only the Early Cretaceous discontinuity *sensu* Lefeld (1968) encompasses merely part of the actual geologic history of the High-Tatric sedimentary zone (most likely the ?latest Tithonian–late Berriasian erosion; compare with Lodowski and Grabowski 2023), but also his sedimentological interpretations should be taken with caution due to stratigraphic inaccuracies.

In a broader context, the large stratigraphical gap in the autochthonous High-Tatric Zone documented in this study might be compared to the Lower Cretaceous hiatus on the Czorsztyn Ridge of the Pieniny Klippen Belt (Text-fig. 1F; e.g. Wierzbowski 1994; Aubrecht *et al.* 2022 and references therein), which was interpreted as being related to extension and rifting in the Magura Ocean (Plašienka 2018). A common effect of subduction in the Neotethyan Collision Belt and rifting in the Penninic oceans was later proposed to explain the latest Jurassic–earliest Cretaceous uplift of the High-Tatric zone, as observed in the Giewont succession (Lodowski and Grabowski 2023); this study provide further evidence of this phenomena.

CONCLUSIONS

- Raptawicka Gate section provides an insight into the Tithonian–Aptian of the High-Tatric succession, with a transition between the Raptawicka Turnia Limestone Formation (RTL Fm) and the Wysoka Turnia Limestone Formation (WTL Fm). The contact between the formations has an erosional character, with an erosional gap spanning the topmost Tithonian–?basal Aptian.
- Microfossil occurrences document the Malmica and ?Tenuis calcareous dinocyst zones, as well as

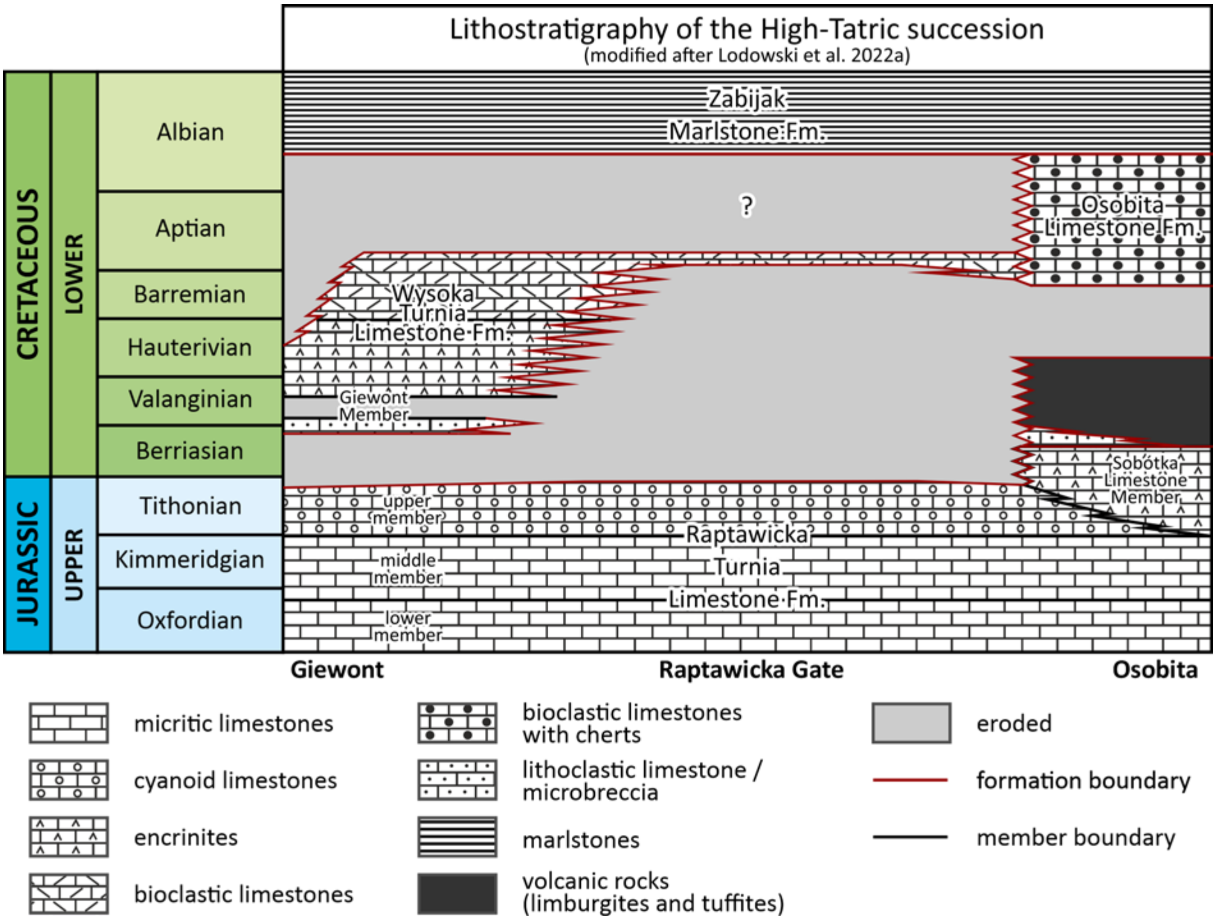

Text-fig. 9. Lithostratigraphy of the High-Tatric succession, modified after Lodowski *et al.* (2022a) with respect to findings of this study. Lithostratigraphy of the Mt. Osobita area after Madzin *et al.* (2014).

the calpionellid Remanei Subzone (Crassicollaria Zone). The foraminiferal assemblage of the WTL Fm (co-occurrence of *Favusella hoterivica* and *Hedbergella hispaniae* among others) suggests the early Aptian age of this interval.

- The most common bioclasts of the RTL Fm are cyanoids, yet important constituents are also *Globochaete alpina* algae, *Saccocoma* sp. (planktic crinoids), other crinoids, radiolarians, and calpionellids. In turn, the WTL Fm interval is dominated by crinoidal fragments (= encrinites), with common admixture of peloids. The occurrence of orbitolinids within the upper part of the section documents the rare High-Tatric "Urgonian" facies.
- Stable carbon isotopes suggests that the WTL Fm interval covers the interval directly predating the OAE 1a event, or the event *sensu largo*, missing however the record a profound drop in $\delta^{13}C$ characteristic for the Selli event, which may fall into the observational gap. Consequently, the Raptawicka Gate section provides the first documented record of the OAE 1a interval from within the High-Tatric succession.
- The stratigraphic gap between the topmost Jurassic and Lower Cretaceous beds in the Raptawicka Gate section (High-Tatric autochthonous cover) is significantly larger (cf. topmost Tithonian–basal Aptian) than in the case of the Giewont succession (Giewont Nappe; cf. topmost Tithonian–Berriasian), which points to the diachronous character of the base of the WTL Fm.
- Microfacial trends, in particular the stepwise demise of *Saccocoma* and a sudden increase in the abundance of calpionellids within the RTL Fm of the Raptawicka Gate section conform with those documented in other Western Tethys successions (i.e. Vocontian Basin, Transdanubian Range and Southern Alps). This suggests that environmental

processes controlling the deposition in the High-Tatric deposition zone (South Tatric ridge) were to large extent supraregional in scale.

Acknowledgements

This research benefited from financial support from Polish Geological Institute–National Research Institute (project no. 61.2308.2300.00.0; leader: D.G. Lodowski) and AGH Subsidy Funds (no. 16.16.140.315; microfossil studies by Anna Waśkowska and Justyna Kowal-Kasprzyk). The authors would also like to express their warmest thanks to the management of the Tatra National Park, Poland (TPN) for allowing them to conduct this research within the protected area. Appendices 1–4 will be available via Zenodo platform upon publication using the following DOI: 10.5281/zenodo.19416815. Critical remarks of R. Jach and D. Reháková (journal reviewers) are gratefully acknowledged.

REFERENCES

Aubrecht, R., Józsa, Š., Plašienka, D., Wierzbowski, H. 2022. Mid-Cretaceous turnover in the Oravic segment of the Pieniny Klippen Belt (Western and Eastern Carpathians): new data and synthesis. *Cretaceous Research*, **140**, 105323.

Basu, H., Mahendra Kumar, K., Paneerselvam, S. and Chaki, A., 2009. Study of provenance characteristics and depositional history on the basis of U, Th, and K abundances in the Gulcheru Formation, Cuddapah basin in Tummalapalle-Somalollapalle areas, Cuddapah-Aanantapur districts, Andhra Pradesh. *Journal of the Geological Society of India*, **74**, 318–328.

Borowska, U., 2015. Stratigraphy of the Lower Tithonian-Lower Aptian limestones of the Niedźwiedź crag from the High-Tatric allochthon, Polish Western Tatra Mountains. *Przegląd Geologiczny*, 63, 164–171. [in Polish with English summary]

BouDagher-Fadel, M.K., 2015. Biostratigraphic and Geological Significance of Planktonic Foraminifera. UCL Press, London, 306 pp.

Calvert, S.E. and Pedersen, T.F., 2007. Elemental proxies for palaeoclimatic and palaeoceanographic variability in marine sediments: Interpretation and application. *Developments in Marine Geology*, **1**, 567–644.

Coccioni, R., Premoli Silva, I., Marsili, A. and Verga, D., 2007. First radiation of Cretaceous planktonic foraminifera with radially elongate chambers at Angles (Southeastern France) and biostratigraphic implications. *Revue de Micropaleontologie*, **50**, 215–224.

Colombie, C., Lécuyer, C. and Strasser, A., 2011. Carbon- and oxygen-isotope records of palaeoenvironmental and carbonate production changes in shallow-marine carbonates (Kimmeridgian, Swiss Jura). *Geological Magazine*, **148**, 133–153.

Cramer, B.D. and Jarvis, I., 2020. Carbon Isotope Stratigraphy. In: Gradstein, F.M., Ogg, J.G., Schmitz, M.D., Ogg, G.M. (Eds) Geologic Time Scale 2020. 309–344. Elsevier, Amsterdam, Oxford, Cambridge.

Erba, E., Channell, J.E.T., Claps, M., Jones, C., Larson, R., Opdyke, B., Premoli Silva, I., Riva, A., Salvini, G. and Torricelli, S., 1999. Integrated stratigraphy of the Cismon APTICORE (Southern Alps, Italy): A “reference section” for the Barremian–Aptian interval at low lattitudes. *Journal of Foraminiferal Research*, **29**, 371–391.

Fedeli, R., Di Lella, L.A. and Loppi, S., 2024. Suitability of XRF for routine analysis of multi-elemental composition: A multi-standard verification. *Methods and Protocols*, **7**, 53.

Frau, C., Bulot, L.G., Delanoy, G., Moreno-Bedmar, J.A., Masse, J.-P., Tendil, A.J.-B. and Lanteaume, C., 2018. The Aptian GSSP candidate at Gorgo a Cerbara (Central Italy): an alternative interpretation of the bio-, litho- and chemostratigraphic markers. *Newsletters on Stratigraphy*, **53**, 311–326.

Gale, A.S., Mutterlose, J. and Batenburg, S., 2020. The Creteceous Period. In: Gradstein, F.M., Ogg, J.G., Schmitz, M.D., Ogg, G.M. (Eds) Geologic Time Scale 2020. 1023–1086. Elsevier, Amsterdam, Oxford, Cambridge.

Grabowski, J. 1997. Paleomagnetic results from the cover (High-Tatric) unit and the nummulitic Eocene in the Tatra Mts (Central West Carpathians, Poland) and their tectonic implications. *Annales Societatis Geologorum Poloniae*, **67**, 13–23.

Grabowski, J., Bakhmutov, V., Kdýr, Š., Krobicki, M., Pruner, P., Rehákova, D., Schnabl, P., Stoykova, K. and Wierzbowski, H., 2019. Integrated stratigraphy and palaeoenvironmental interpretation of the Upper Kimmeridgian to Lower Berriasian pelagic sequences of the Velykyi Kamianets section (Pieniny Klippen Belt, Ukraine). *Palaeogeography, Palaeoclimatology, Palaeoecology*, **532**, 109216.

Grabowski, J., Chmielewski, A., Ploch, I., Rogov, M., Smoleń, J., Wójcik-Tabol, P., Leszczyński, K. and Maj-Szeliga, K., 2021a. Palaeoclimatic changes and inter-regional correlations in the Jurassic/Cretaceous boundary interval of the Polish-Basin: portable XRF and magnetic susceptibility study. *Newsletters on Stratigraphy*, **54**, 123–158.

Grabowski, J., Stoykova, K., Wierzbowski, H. and Wójcik-Tabol, P., 2021b. Upper Berriasian chemostratigraphy, clay minerals and calcareous nannofossils of the Barlya section (Western Balkan, Bulgaria): implications for paleoclimate and productivity changes, and stratigraphic correlations across the Alpine Tethys. *Palaeogeography, Palaeoclimatology, Palaeoecology*, **567**, 110252.

Grabowski, J., Bąk, K., Bąk, M., Krobicki, M., Lodowski, D., Uchman, A., Golonka, J., Górny, Z., Hejnar, J., Iwańczuk, J., Olszewska, B., Oszczypko, N., Salata, D., Wierzbowski, A. and Wójcik-Tabol, P., 2022. From shallow to deep marine depositional environments of the Cretaceous northwestern Tethys – a record of Alpine system differentiation in the Polish Carpathians. In: Walaszczyk, I., Todes J.P. (Eds) Cretaceous of Poland and adjacent areas: Field trip guides. 11th International Cretaceous Symposium, Warsaw, Poland, 2022. 297–362, 406 p. University of Warsaw, Warsaw.

Grabowski, J., Lodowski, D.G., Pszczółkowski, A., Chadimová, L., Császár, G., Sobień, K. and Szinger, B., 2024. Palaeoenvironmental indices (calpionellids, gagmma-ray spectrometry, magnetic susceptibility) in the Berriasian of the Tisza mega-unit (Lipse-tető, Mecsek Mts, Hungary) and the Central Western Carpathians (lower Sub-Tatric succession, Tatra Mts, Poland) – a comparison. *Acta Geologica Polonica*, **74**, e27.

Grabowski, J., Pszczółkowski, A., Stoykova, K., Martinez, M., Iwańczuk, J., Krzemiński, L. and Sidorczuk, M., 2025. Integrated stratigraphy of the Valanginian Carbon-Isotope-Excursion (Weissert event) from the Kryta Valley section, Western Carpathians (Poland): correlation with the Vocontian Basin and palaeoenvironmental implications. *Newsletters on Stratigraphy*, **58**, 1–46.

Granier, B., Clavel, B., Busnardo, R., Charollais, J., Desjacques, P. and Bert, D., 2021. Biostratigraphic distribution of orbitolinids in the ammonite biozones (Urgonian platform of southeastern France). Part 2: Barremian p.p. *Carnets de Géologie*, **21**, 399–521.

Häusler, H., Plašienka, D. and Polák, M., 1993. Comparison of Mesozoic successions of the Central Eastern Alps and the Central Western Carpathians. *Jahrbuch der Geologischen Bundesanstalt*, **136**, 715–739.

Herrle, J.O., Schröder-Adams, C.J., Davis, W., Pugh, A.T., Galloway, J.M. and Fath, J., 2015. Mid-Cretaceous High Arctic stratigraphy, climate, and Oceanic Anoxic Events. *Geology*, **43**, 403–406.

Hesselbo, S.P., Ogg, J.G., and Ruhl, M., 2020. The Jurassic Period. In: Gradstein, F.M., Ogg, J.G., Schmitz, M.D. and Ogg, G.M. (Eds), The Geologic Time Scale 2020, 955–1022. Elsevier; Amsterdam, London, Cambridge.

Huber, B.T. and Leckie, R.M., 2011. Planktic foraminiferal species turnover across deep-sea Aptian/Albian boundary sections. *Journal of Foraminiferal Research*, **41**, 53–95.

Jurewicz, E., 2005. Geodynamic evolution of the Tatra Mts. And the Pieniny Klippen Belt (Western Carpathians): problems and comments. *Acta Geologica Polonica*, **55**, 295–338.

Kotański, Z. 1971. Przewodnik geologiczny po Tatrach. Wydawnictwa Geologiczne, Warszawa, 1971. 280 pp.

Lakova, I. and Petrova, S., 2013. Towards a standard Tithonian to Valanginian calpionellids zonation of the Tethyan Realm. *Acta Geologica Polonica*, **63**, 201–221.

Lefeld, J., 1968. Stratigraphy and palaeogeography of the High-Tatric Lower Cretaceous in the Tatra Mountains. *Studia Geologica Polonica*, **24**, 1–115. [In Polish with English summary]

Lefeld, J., Gaździcki, A., Iwanow, A., Krajewski, K. and Wójcik, K., 1985. Jurassic and Cretaceous lithostratigraphic units of the Tatra Mountains. *Studia Geologica Polonica*, **84**, 7–93.

Lipson-Benitah, S. and Almogi-Labin, A., 2004. Aptian planktonic foraminifera from Israel. *Israel Journal of Earth Sciences*, **53**, 27–46.

Lodowski, D.G. and Grabowski, J., 2023. Tracing the latest Jurassic–earliest Cretaceous paleoenvironment evolution in swell carbonate facies: a case study of the High-Tatric succession (Central Western Carpathians, Tatra Mts, Poland). *Acta Geologica Polonica*, **73**, 741–772.

Lodowski, D.G., Pszczółkowski, A., Wilamowski, A. and Grabowski, J., 2022a. The Jurassic–Cretaceous transition in the High-Tatric succession (Giewont Unit, Western Tatra Mts, Poland): integrated stratigraphy and microfacies. *Acta Geologica Polonica*, **72**, 107–135.

Lodowski, D.G., Pszczółkowski, A., Szives, O., Főzy, I. and Grabowski, J,. 2022b. Jurassic–Cretaceous transition in the Transdanubian Range (Hungary): integrated stratigraphy and paleomagnetic study of the Hárskút and Lókút sections. *Newsletters on Stratigraphy*, **55**, 99–135.

Lodowski, D.G., Szives, O., Virág, A. and Grabowski J., 2024a. The latest Jurassic–earliest Cretaceous climate and oceanographic changes in the Western Tethys: The Transdanubian Range (Hungary) perspective. *Sedimentology*, **71**, 1843–1872.

Lodowski, D.G., Grabowski, J., Rožič, B., Žvab-Rožič, P., Reháková, D., Slapnik, L., Iwańczuk, J., Chmielewski, A. and Teodorski, A., 2024b. The Jurassic–Cretaceous transition in the Slovenian Basin (Alpine Atlantic): Further evidence for palaeoenvironmental record in pelagic sediments. *Geochemistry, Geophysics, Geosystems*, **25**, e2024GC011728.

Lodowski, D.G., Schnyder, J., Kowal-Kasprzyk, J., Deconinck, J.-F., Martinez, M., Chmielewski, A., Ploch, I. and Grabowski, J., 2025. Climate changes at the Jurassic/Cretaceous transition vs. supra-regional oceanographic processes: Insights from the Vocontian Basin (Clue de Taulanne section, SE France). *Global and Planetary Change*, **252**, 104836.

Madzin, J., Sýkora, M. and Soták, J., 2014. Stratigraphic position of alkaline volcanic rocks in the autochthonous cover of the High-Tatric Unit (Western Tatra Mts., Central Western Carpathians, Slovakia). *Geological Quarterly*, **58**, 163–180.

Masse, J.P. and Uchman, A., 1997. New biostratigraphic data on the Early Cretaceous platform carbonates of the Tatra Mountains, Western Carpathians, Poland. *Cretaceous Research*, **18**, 713–729.

Michalík, J. 1994. Lower Cretaceous carbonate platform facies, Western Carpathians. *Palaeogeography, Palaeoclimatology, Palaeoecology*, **111**, 263–277.

Michalík, J. and Soták, J. 1990. Lower Cretaceous shallow marine buildups in the Western Carpathians and their relationship to pelagic facies. *Cretaceous Research*, **11**, 211–227.

Mišík, M. 1966. Microfacies of the Mesozoic and Tertiary limestones of the West Carpathians. 279 p. Vydavateľstwo Slovenskej Akadémie Vied, Bratislava.

Mišík, M. and Reháková, D., 2009. Vápence Slovenska – I. časť (biohermné, krinoidové, sladkovodné, ooidové a onkoidové vápence). Limestones VEDA, 186 p. [in Slovak]

Moore, C.H. 2001. Carbonate Reservoirs: Porosity evolution and diagenesis in a sequence stratigraphic framework, 460 pp. Elsevier; Amsterdam.

Möller, C., Bornemann, A. and Mutterlose, J., 2020. Climate and paleoceanography controlled size variations of calcareous nannofossils during the Valanginian Weissert Event (Early Cretaceous). *Marine Micropaleontology*, **157**, 101875.

Nemčok, J., Bezák, V., Biely, A., Gorek, A., Gross, P., Halouzka, R., Janák, M., Kahan, Š., Kotański, Z., Lefeld, J., Mello, J., Reichwalder, P., Rączkowski, W., Roniewicz, P., Ryka, W., Wieczorek, J. and Zelman, J., 1994. Geological map of the Tatra Mountains. MŽP SR, GÚDŠ; Bratislava.

Ölveczká, D. and Reháková, D., 2022. Upper Tithonian Crassicollaria Zone: new data on the calpionellid distribution and subzonal division of the Pieniny Klippen Belt in the Western Carpathians. *Acta Geologica Slovaca*, **14**, 37–56.

Petrizzo, M.R., King, D.J., Pearson, P.N., Huber, B.T. and Wade, B.S., 2024. Planktonic foraminifera in biostratigraphy and biochronology. *Newsletters on Stratigraphy*, **2024**, 106050.

Petrova, S., Reháková, D., Erba, E. and Grabowski, J., 2025. Tithonian–Berriasian calpionellid and calcareous dinocyst biostratigraphy, and microfacies in the Torre de' Busi section (Lombardian Basin, northern Italy). *Cretaceous Research*, **176**, 106180.

Piotrowski J. 1978. Mesostructural analysis of the main tectonic units of the Tatra Mountains along the Kościeliska Valley. *Studia Geologica Polonica*, **55**, 3–90. [In Polish with English summary]

Plašienka, D., 2018. Continuity and episodicity in the early Alpine tectonic evolution of the Western Carpathians: How large-scale processes are expressed by the orogenic architecture and rock record data. *Tectonics*, **37**, 2029–2079.

Premoli Silva, I. and Verga, D., 2004. Practical Manual of Cretaceous Planktonic Foraminifera. International School on Planktonic Foraminifera: 3rd Course: Cretaceous: Perugia, 16–20 February 2004. Universities of Perugia and Milano, Tipografia Ponte Felcino, Perugia, Italy, 283 pp.

Pszczółkowski, A., 1996. Calpionellid stratigraphy of the Tithonian-Berriasian pelagic limestones in the Tatra Mts (Western Carpathians). *Studia Geologica Polonica*, **109**, 103–130.

Pszczółkowski, A., 2003. Kościeliska Marl Formation (Lower Cretaceous) in the Polish Western Tatra Mountains: lithostratigraphy and microfossil zones. *Studia Geologica Polonica*, **121**, 7–50.

Pszczółkowski, A., 2015. Aptian foraminiferal stratigraphy and Nannoconus assemblages from the Kopka section (Western Tatra Mountains, Poland). *Annales Societatis Geologorum Poloniae*, **85**, 123–138.

Pszczółkowski, A., 2018. Upper Jurassic bacteria from the Raptawicka Turnia Limestone Formation in the Mały Giewont area (Western Tatra Mountains, Poland). *Geological Quarterly*, **62**, 840–857.

Pszczółkowski, A., Grabowski, J. and Wilamowski, A., 2016. Integrated biostratigraphy and carbon isotope stratigraphy of the Upper Jurassic shallow water carbonates of the High-Tatric Unit (Mały Giewont area, Western Tatra Mountains, Poland). *Geological Quarterly*, **60**, 893–918.

Qin, Z., Xi, D., Wagreich, M., Sames, B., Tong, X., Hu, J. and Wan, X., 2021. Living environment of the early Jehol Biota: A case study from the lower Cretaceous Dabeigou Formation, Luanping Basin (North China). *Cretaceous Research*, **124**, 104833.

Reháková, D., 2000. Evolution and distribution of the late Jurassic and early Cretaceous calcareous dinoflagellates recorded in the Western Carpathian pelagic carbonate facies. *Mineralia Slovaka*, **32**, 79–88.

Schneider, R.R., Price, B., Müller, P.J., Kroon, D. and Alexander, I., 1997. Monsoon related variations in Zaire (Congo) sediment load and influence of fluvial silicate supply on marine productivity in the east equatorial Atlantic during the last 200,000 years. *Paleoceanography*, **12**, 463–481.

Simmons, M. D. and Williams, C. L., 1992. Cretaceous Orbitolinidae (Foraminifera) from onshore and offshore southwest England. *Journal of Micropaleontology*, **11**, 21–30.

Szczegółowa Mapa Geologiczna Tatr 1:10 000. Państwowy Instytut Geologiczny – Państwowy Instytut Badawczy, 2022. https://geologia.pgi.gov.pl/smgt/

Tian, J., Xie, X., Ma, W., Jin, H. and Wang, P., 2011. X-ray fluorescence core scanning records of chemical weathering and monsoon evolution over the past 5 Myr in the southern South China Sea. *Paleoceanography*, **26**, PA4202.

Wei, G., Liu, Y., Li, X., Shao, L. and Liang, X., 2003. Climatic impact on Al, K, Sc, and Ti in marine sediments: Evidence from ODP Site 1144, South China Sea. *Geochemical Journal*, **37**, 593–602.

Wierzbowski, A. 1994. Late Middle to earliest Cretaceous stratigraphy and microfacies of the Czorsztyn Succession in the Spisz area, Pieniny Klippen Belt, Poland. Acta Geologica Polonica, 44, 3–4, 223–249.

Manuscript submitted: 19th February 2026
Revised version accepted: 20th May 2026

PLATES 1–3

PLATE 1

Tithonian calcareous dinocysts and calpionellids in the Raptawicka Gate section.

A – *Parastomisphaera malmica* (Borza) (sample BK1).

B – *Parastomisphaera malmica* (Borza) (BK2).

C – *Colomisphaera carpathica* (Borza) (BK11).

D – *Colomisphaera cieszynica* Nowak (BK8).

E – *Committosphaera* cf. *pulla* (Borza) (BK1).

F – *Colomisphaera* cf. *tenuis* (Nagy) (BK8).

G – *Tintinnopsella remanei* Borza (BK170).

H – *Tintinnopsella carpathica* (Murgeanu et Filipescu) (BK189).

I – *Crassicollaria intermedia* (Durand Delga) (BK183).

J – *Crassicollaria intermedia* (Durand Delga) (BK185);

K – *Crassicollaria brevis* Remane (BK185).

L – *Crassicollaria brevis* Remane (BK193).

M – *Crassicollaria colomi* Doben (BK181).

N – *Crassicollaria massutiniana* (Colom) – oblique section (BK187).

O – *Crassicollaria parvula* Remane (BK187).

P – *Calpionella alpina* Lorenz (BK187).

All specimens are from the Raptawicka Turnia Formation of the High-Tatric succession

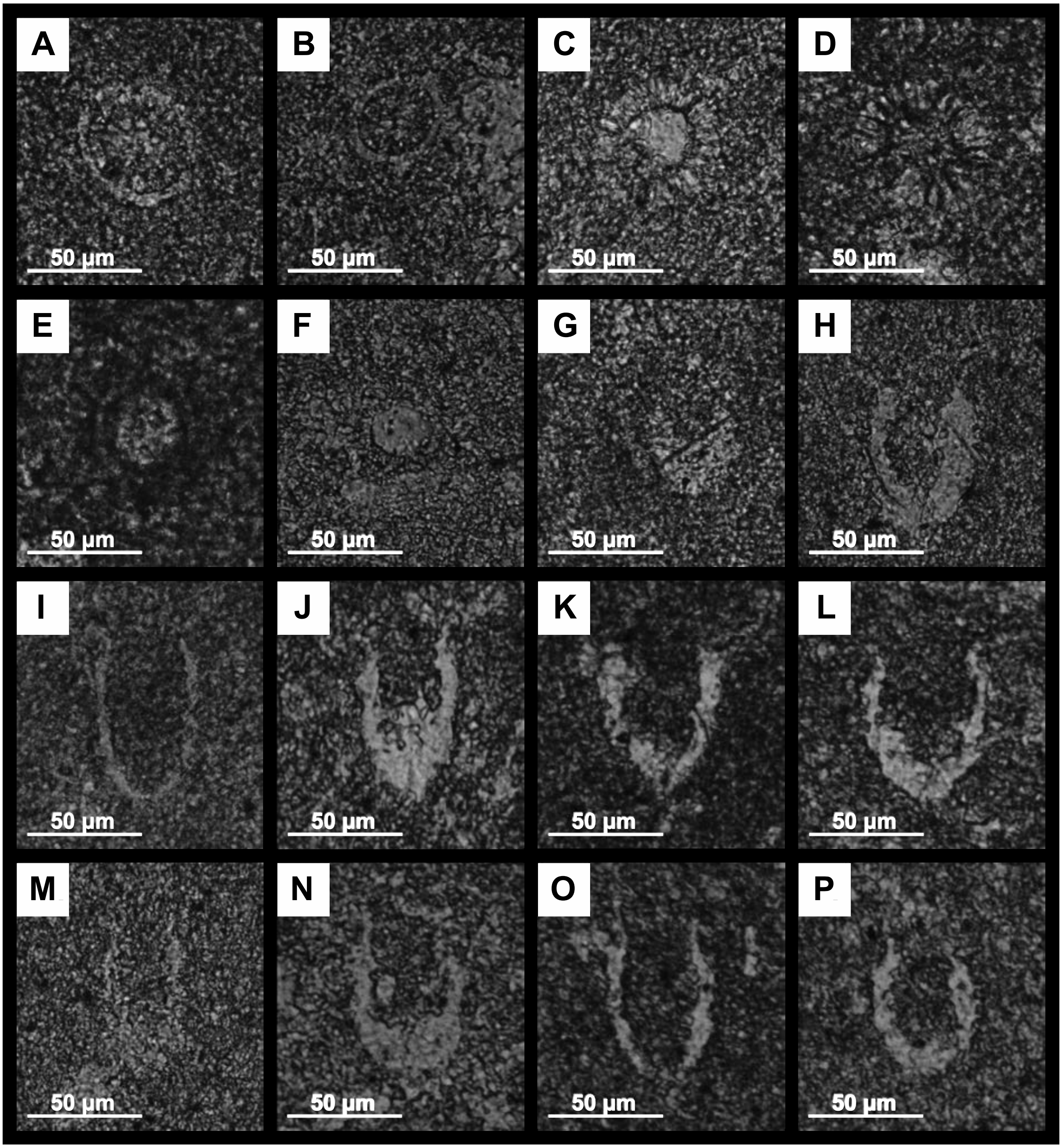
A
50 µm
B
50 µm
C
50 µm
D
50 µm
E
50 µm
F
50 µm
G
50 µm
H
50 µm
I
50 µm
J
50 µm
K
50 µm
L
50 µm
M
50 µm
N
50 µm
O
50 µm
P
50 µm

PLATE 2

Benthic foraminifera (and red algae) in the upper part of the Raptawicka Gate section.

A – *Protopenerolis banatica* Bucur (sample BK 210).

B, **C** – indeterminate red algae (B: BK 208; C: BK 210).

D – textulariid (biserial): *Gaudryina* sp. (BK 210).

E, **I**–**K** – *Nezzazata isabellae* Arnaud-Vanneau et Sliter (E: BK 212, I: BK 208, J: BK 199, K: BK201).

F, **G** – *Sabaudia minuta* (Hofker) (F: BK 197, G: BK 210).

H – textulariid (biserial): *Dorothia* sp. (BK 205).

L – *Glomospira* sp. (BK 210).

M – *Conorboides* sp. (BK 212).

All specimens are fromthe Wysoka Turnia Formation of the High-Tatric succession.

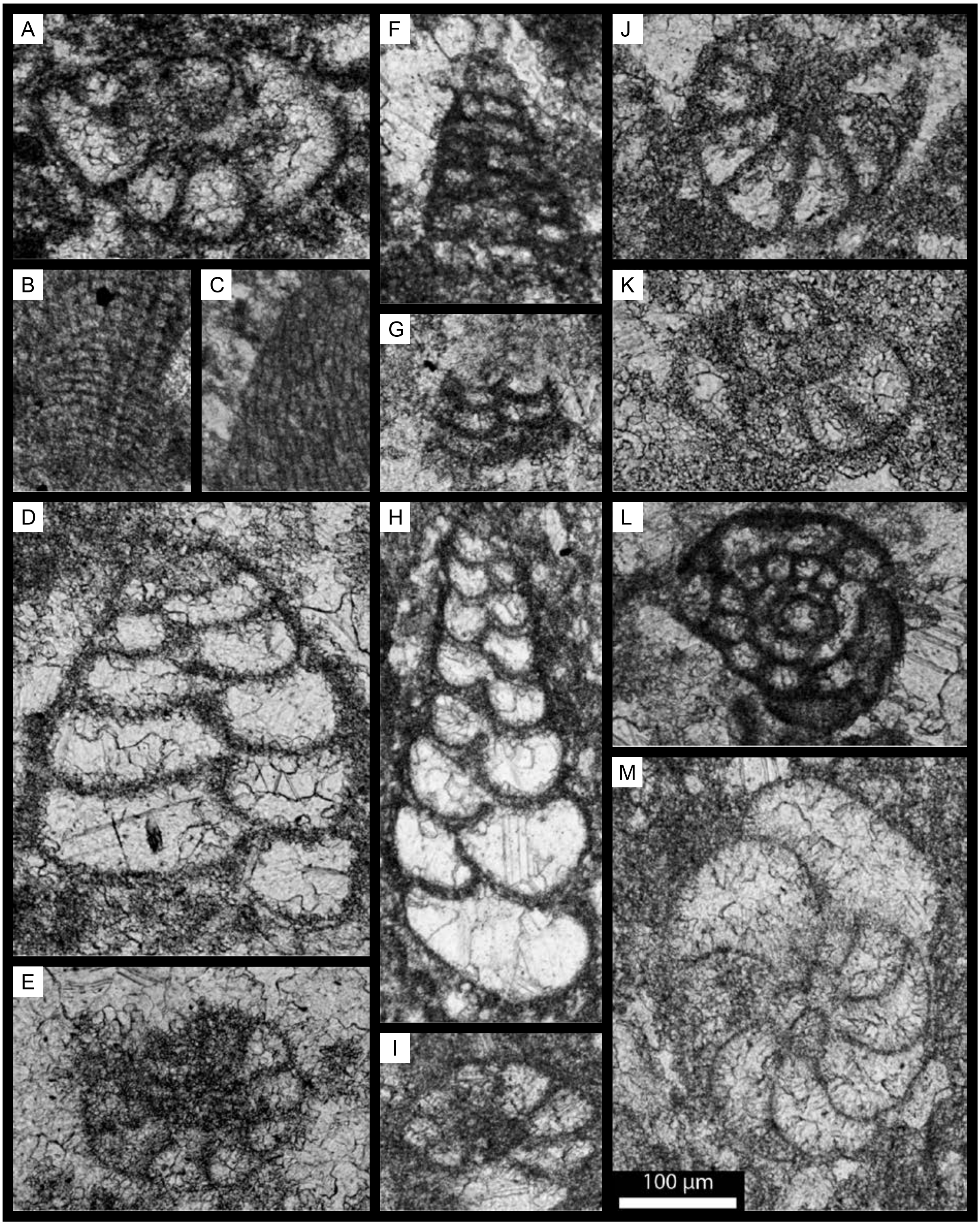
A
B
C
D
E
F
G
H
I
J
K
L
M
100 µm

PLATE 3

Planktic foraminifera in the upper part of the Raptawicka Gate section.

A, **B** – *Favusella hoterivica* (Subbotina) (A: sample BK199; B: sample BK197).

C – *Globigerinelloides ?* cf. *barri* (Bolli *et al.*) (sample BK199).

D – *Globigerinelloides blowi* (Bolli) (BK197).

E – *Globigerinelloides aptiensis* Longoria (BK197).

F – *Globigerinelloides aptiensis* Longoria (BK199).

G – *Globigerinelloides paragottisi* Verga et Premoli Silva (BK199).

H – *Hedbergella praetrocoidea* Kretchmar et Gorbachik (BK199).

I – *Hedbergella luterbacheri* Longoria (BK199).

J – *Hedbergella infracretacea* (Glaessner) (BK212).

K – *Hedbergella tardita* (Antonova) (BK212).

L – *Hedbergella semielongata* Longoria (BK196).

M – *Hedbergella hispaniae* Longoria (BK212).

N – *Hedbergella sigali* Moullade (BK210).

O – *Hedbergella occulta* Longoria (BK196).

All specimens are fromthe Wysoka Turnia Formation of the High-Tatric succession.

Scale bars equal 100 μm.

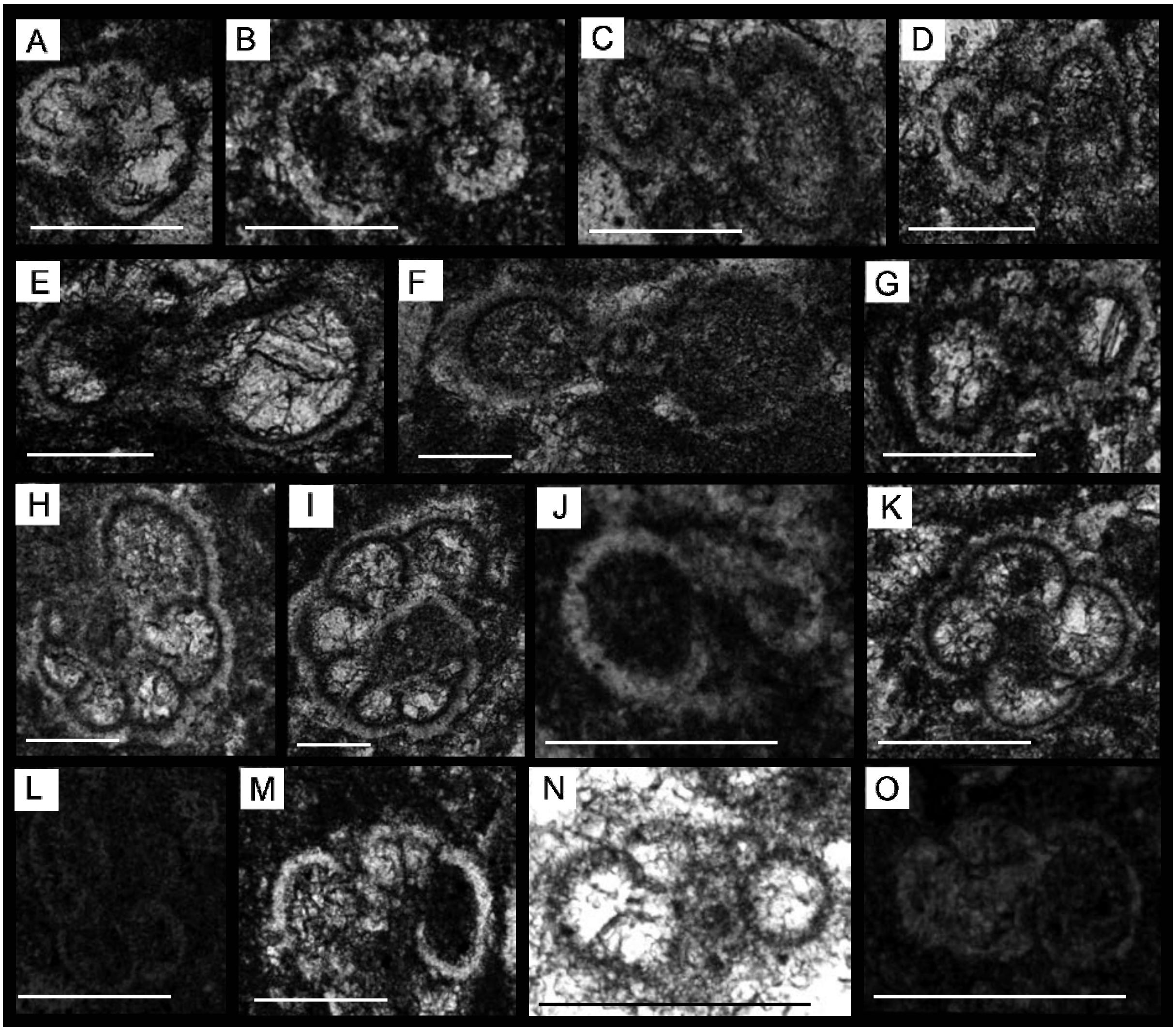
A
B
C
D
E
F
G
H
I
J
K
L
M
N
O